Received: 25 March 2025 | Revised: 8 July 2025 | Accepted: 29 July 2025

DOI: 10.1002/dep2.70037

The Depositional Record
Open Access
A journal of the International Association of Sedimentologists
IAS
WILEY

ORIGINAL ARTICLE

Black shale deposition during the Early Jurassic: Geochemistry of Pliensbachian and Toarcian sedimentary rocks of the Hunzen Well, Hils Syncline, Northwest German Basin

Premila Wijesinghe[1] | **Ralf Littke**[1] | **Linda Burnaz**[1] | **Martin Blumenberg**[2] | **Jochen Erbacher**[2] | **Thomas Mann**[2] | **Florian Amann**[3] | **Thorsten Bauersachs**[1]

[1]Institute for Organic Biogeochemistry in Geo-Systems, Energy and Mineral Resources Group (EMR), RWTH Aachen University, Aachen, Germany

[2]Federal Institute for Geosciences and Natural Resources (BGR), Hannover, Germany

[3]Chair of Engineering Geology and Hydrogeology, RWTH Aachen University, Aachen, Germany

Correspondence
Premila Wijesinghe, Institute for Organic Biogeochemistry in Geo-Systems, Energy and Mineral Resources Group (EMR), RWTH Aachen University, Aachen, Germany.
Email: premila.wijesinghe@emr.rwth-aachen.de

Funding information
German Federal Ministry for Economic Affairs and Climate Action (BMWK), MATURITY project, Grant/Award Number: 02E11931

Abstract

The Toarcian stage of the Early Jurassic witnessed warm global temperatures, oceanic anoxia (Toarcian Oceanic Anoxic Events) and extensive deposition of organic-rich black shales. While black shale deposition in the Southwest German Basin on the Northwest Tethyan shelf has been well-studied, the palaeodepositional conditions in the Northwest German Basin remain poorly constrained. The present study aims to bridge that gap by examining a completely cored well covering Upper Pliensbachian to Upper Toarcian sediments in the Hils Syncline. Inorganic and organic geochemical, as well as biostratigraphic information, carbon isotope and organic petrological results are interpreted to reconstruct depositional conditions and organic matter accumulation in a shallow Jurassic Sea. The study results demonstrate a Late Pliensbachian regression leading to the deposition of claystone in shallow water under humid conditions with a high terrigenous and freshwater influx, and well-oxygenated bottom water environments. A transgression in the Early Toarcian initiated the deposition of laminated and organic matter-rich calcareous black shale, the so-called Posidonia Shale. This climatic shift caused deepening of the water column, resulting in salinity stratification and bottom water anoxia that favoured organic matter preservation. Black shale deposition was probably triggered by low oxygen solubility in warm waters and intensified monsoonal rainfall. The lowermost part of the Posidonia Shale (basal Unit I) represents the time of most intense carbonate deposition and strictly anoxic bottom water. The middle part (Unit II) is characterised by periodical, short-term oxygenation of the sea floor, while the thick upper part (Unit III) represents a time of re-establishment of anoxic conditions. In the Late Toarcian and Aalenian, bottom water reoxygenation marked the deposition of claystones with moderate contents of marine organic matter, above a decimetre-thick breccia. The Hunzen section thus offers

detailed insights into late Early to Middle Jurassic palaeodepositional changes in central Europe.

KEYWORDS

black shales, geochemistry, Lower Jurassic, oceanic anoxic event, Pliensbachian, Posidonia Shale, Toarcian

1 | INTRODUCTION

1.1 | General context and objectives

The Toarcian stage (184.2 to 174.7 Ma) was characterised by significant environmental perturbations, including massive magmatism, marine mass extinctions, an oceanic anoxic event (OAE), water mass exchange limitations, rapid global warming and sea level variations (Harries & Little, 1999; Jenkyns, 1988; Pálfy & Smith, 2000; Wignall et al., 2005). These climatic and environmental instabilities during the Toarcian had a profound impact on the depositional conditions at shallow shelf areas, resulting in the widespread deposition of organic-rich (>10 wt%) black shales (Hesselbo et al., 2000; Jenkyns, 2010; Küspert, 1982; McArthur et al., 2008; van de Schootbrugge et al., 2005; Wang et al., 2021). Black shale deposition occurred across the European archipelago with the most extensive deposition on the continental margins of the Tethys as well as epicontinental shelf areas (Ziegler, 1990).

The global and regional mechanisms governing Early Toarcian black shale deposition have been extensively studied over the past decades, but are still controversially debated. Black shale deposition is intimately associated with the Toarcian Oceanic Anoxic Event (T-OAE) (Hesselbo et al., 2000; Jenkyns, 2010; Ruebsam et al., 2022; Thibault et al., 2018), which is characterised by the global spread of bottom water anoxia and a negative carbon isotope excursion (nCIE) of organic matter (Hesselbo et al., 2000, 2007). The excursion, which is explained by the release of isotopically light carbon (^{12}C) into the atmosphere, indicates significant global carbon cycle perturbations, probably linked to the Karoo-Ferrar Large Igneous Province (KFLIP) massive volcanism (Svensen et al., 2007; van de Schootbrugge et al., 2005; Wignall, 2001) and the thermogenic dissociation of methane hydrate from marine sediments (Hesselbo et al., 2000; Kemp et al., 2005; Them, Gill, Caruthers, et al., 2017; van de Schootbrugge et al., 2005) and the potential release of cryogenic carbon from thawing permafrost and peatlands (Ruebsam et al., 2019). Besides this widely accepted T-OAE hypothesis, some studies have advocated alternative explanations for black shale deposition, including a transgression across hydrographically restricted basins with distinct swell topography (Frimmel et al., 2004; Küspert, 1982; McArthur et al., 2008). Such a transgression may have favoured conditions conducive to black shale formation independently of a global OAE. More recent studies also render the T-OAE theory more questionable due to (i) the absence of organic-rich sediments in distal oceanic basins, for example, Western Tethys in present-day Southern Europe and Northern Africa (Hesselbo et al., 2007; Silva et al., 2021) and (ii) the observation that the majority of black shales are stratigraphically younger and have been deposited after the nCIE (Burnaz et al., 2024). This suggests that local or regional factors might indeed have played a significant role in black shale formation.

The Early Toarcian organic-rich black shales in the Central European Basin System (CEBS) have attracted considerable scientific interest because they are well-known petroleum source rocks (Littke et al., 1991; Röhl & Schmid-Röhl, 2005; Song et al., 2017). Interestingly, black shale deposition in the CEBS does not appear to have started simultaneously in the various sub-basins (Song et al., 2015; Wignall, 1991). The Posidonia Shale in northern Germany gained particular attention for reconstructing the depositional environment due to its high and rather uniform organic matter (OM) content (5–15 wt% TOC) and thickness which often exceeds 30 m (Röhl et al., 2001; Rullkötter et al., 1988).

Previous geochemical, sedimentological and palaeontological investigations of black shale deposits suggest that their accumulation was associated with profound oceanographic, climatic and depositional perturbations such as elevated atmospheric pCO_2 and intensified greenhouse conditions, enhanced continental weathering and changes in sedimentary dynamics, and significant bottom water warming and thermocline shoaling as reconstructed from palaeothermometric data (Cohen et al., 2004; Hesselbo et al., 2007; McElwain et al., 2005; Ruebsam et al., 2020; Wignall et al., 2005). To explain these, several depositional models have been proposed, considering regional and global factors separately, focusing on greenhouse effects, storm events, eustatic sea-level changes, hydrological cycling and hydrological restriction via salinity stratification

(Frimmel et al., 2004; Küspert, 1982; Röhl et al., 2001; Sælen et al., 2000; van de Schootbrugge et al., 2005). In contrast, more recently proposed scenarios invoke a combination of regional and global driving forces that led to the global black shale deposition of the Toarcian (Burnaz et al., 2024; Fantasia et al., 2018, 2019; Kemp et al., 2022; Remírez & Algeo, 2020; Song et al., 2015, 2017). More precisely, the variation of intensity and timing of bottom water anoxia and black shale deposition largely depended on sea water temperature, nutrient supply, topographical restrictions and eustatic transgression-regression (T/R) cycles (Küspert, 1982; Röhl & Schmid-Röhl, 2005).

Detailed studies of the late Pliensbachian (192.9 ± 0.3 to 184.2 ± 0.3 Ma) to early Toarcian (184.2 to 174.7 ± 0.8 Ma) depositional environment in the Southwest German Basin (SWGB) have yielded valuable insights into past sea-level variations, palaeo water depths and the spatiotemporal distribution of bottom water anoxia and their role in black shale formation (Ajuaba et al., 2022; Frimmel et al., 2004; Röhl et al., 2001; Röhl & Schmid-Röhl, 2005; Schwark & Frimmel, 2004; Song et al., 2017).

In contrast, the Northwestern German Basin (NWGB), despite having thicker and more complete sedimentary sequences (Lokhorst et al., 1996), remains significantly understudied. Prior investigations of the NWGB have focused predominantly on a limited number of borehole profiles mainly from the southern margin and Hils Syncline (Celestino et al., 2024; Gaus et al., 2022; Littke et al., 1991; van de Schootbrugge et al., 2019; Zimmermann et al., 2015). Recently, Ruebsam et al. (2024) conducted a transect-based study covering sites from the Isle of Rügen to Schandelah, providing new insights into regional variability, while additional outcrop-based studies at Marienburg (Loh et al., 1986) and Hondelage (Marten et al., 2024; Mutterlose et al., 2022) further expand the spatial understanding of the NWGB stratigraphy. Most of these studies primarily addressed the thermal maturation and hydrocarbon generation from the organic matter (Fang et al., 2019; Gaus et al., 2022; Sundararaman et al., 1993) due to the economic significance of black shales as petroleum source rocks (Rullkötter et al., 1988).

In the present study, data from a 101 m-thick Upper Pliensbachian to Upper Toarcian sedimentary sequence from the stratigraphically well-defined Hunzen Well, Hils Syncline, Lower Saxony Basin (Northern Germany), are presented. The objective of this study was to develop a coherent model for the changing depositional conditions during the Pliensbachian and Toarcian in the NWGB, considering both global and regional factors. Utilising a multidisciplinary approach, incorporating organic and inorganic geochemistry, carbon isotope geochemistry, organic petrography and biostratigraphical observations (i.e. microfossils), this study offers novel insights into black shale deposition during the Pliensbachian/Toarcian transition in the NWGB, providing stratigraphic information from a yet understudied region of the CEBS.

1.2 | Geological setting

The CEBS, a prominent epicontinental basin structure in central Europe, extends from England to Poland and is bounded by the Sorgenfrei-Tornquist Zone to the north and the Variscan mountains to the south (Scheck-Wenderoth & Lamarche, 2005). The CEBS formed during the Permian through intense magmatism and lithospheric destabilisation from the breakup of Pangea, evolving through extensional tectonics and lithospheric stretching from the Late Carboniferous to the Early Cenozoic (van Wees et al., 2000; Ziegler, 1990) (Figure 1A). During the Permian to Triassic, the CEBS was structured into several sub-basins (Betz et al., 1987; Littke et al., 2008; van Wees et al., 2000), which were separated by shoals, swells and islands (Scheck-Wenderoth & Lamarche, 2005) and show similar evolution with respect to subsidence and sedimentary filling. During this period, mainly continental and shallow marine sediments such as claystone, sandstone, coal and evaporites were deposited (Gaupp et al., 1998; Meschede & Warr, 2019).

During the Early Jurassic, the CEBS was covered by a shallow, epicontinental sea located between 20° and 40° N palaeolatitude. It experienced deposition of diverse lithologies, including predominant shallow marine fine-grained as well as coarse-grained siliciclastics, paralic sediments, and carbonates (Figure 1A,B; Röhl & Schmid-Röhl, 2005). Sea-level rise and water density stratification occurred due to the influx of marine waters through the Arctic seaway (Viking Corridor), while the water mass exchange was limited in deeper sub-basins due to numerous islands and swells (Ziegler, 1990).

During the Middle and Late Jurassic, marine sedimentation continued, but clay-rich fine-grained siliciclastics became successively replaced by coarser-grained sediments and carbonates at the basin's margins (Stollhofen et al., 2008). During the Late Tithonian and Early Berriasian, a transition to paralic, often lacustrine sedimentation took place, followed again by shallow marine sedimentation during the Early Cretaceous (Meschede & Warr, 2019).

The Lower Saxony Basin (LSB) is a sub-basin situated in the western part of the CEBS, bordered by the Rhenish Massif and the Münsterland Basin in the south (Figure 1B). The Hils Syncline as part of the LSB formed due to NE–SW-directed compression during Late Cretaceous inversion tectonics and exhibits a highly variable thermal maturity for Lower Jurassic strata increasing

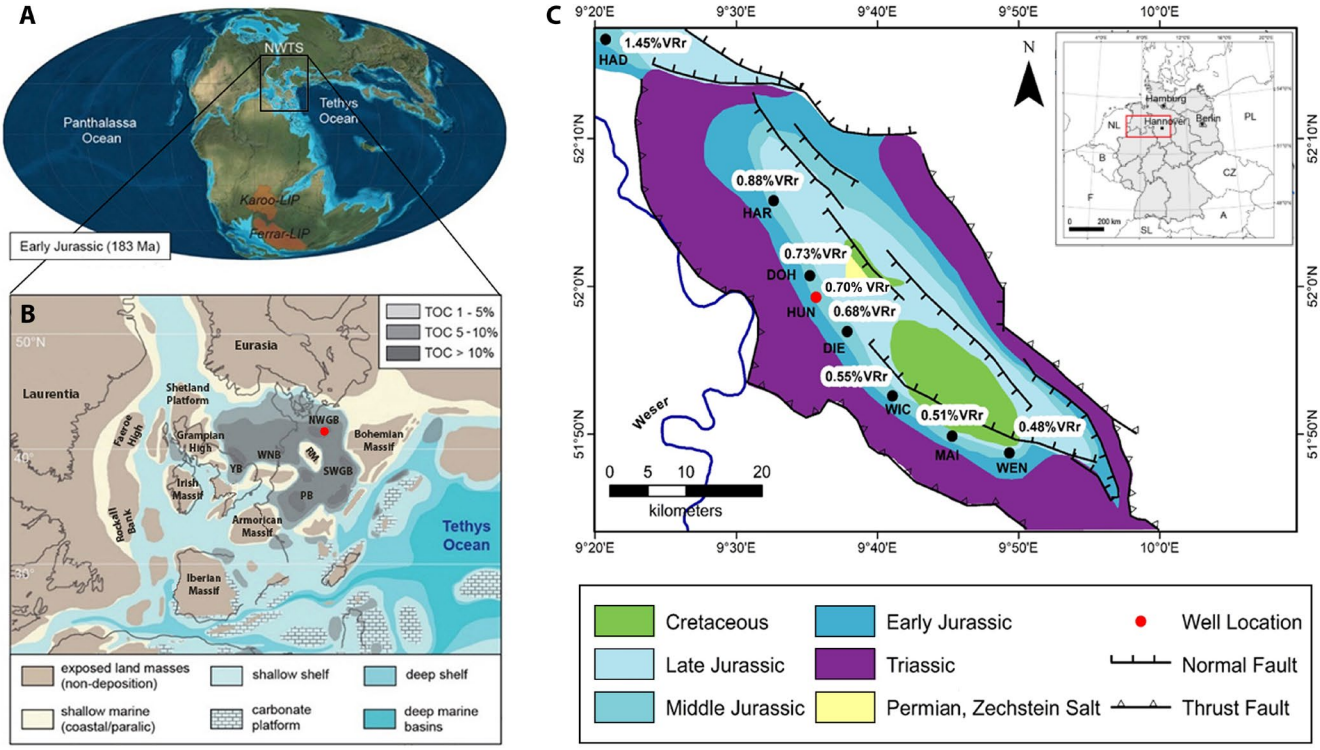

FIGURE 1 (A) Early Jurassic (Toarcian) global palaeogeography after Ruebsam et al. (2022); (B) Palaeogeography of the Central European Basin System (CEBS) with the position of important sub-basins indicated. Red circle shows the position of the Hunzen Well in the Northwest German Basin (NWGB); PB, Paris Basin; WNB, Western Netherland Basin; SWGB, Southwest German Basin; YB, Yorkshire Basin; RM, Rhenish Massif (modified after Ziegler, 1990); (C) Geological map of the Hils Syncline, NW Germany, showing the distribution of Mesozoic strata and major fault systems. The Hunzen Well (HUN) is marked by the red circle. Black circles represent other wells drilled in the Hils Syncline and they are plotted together with vitrinite reflectance (VRr) values of Toarcian claystones. HAD, Haddesen; HAR, Harderode; DOH, Dohnsen; DIE, Dielmissen; WIC, Wickensen; MAI, Mainzholzen and WEN, Wenzen (modified after Fang et al., 2019; Gaus et al., 2022).

from south-east to north-west (0.48–1.45% vitrinite reflectance) over only a short-distance (<70 km) (Figure 1C; Littke et al., 1991).

1.3 | Lithostratigraphic overview

Early to Middle Jurassic sediments of the NWGB consist of marine claystones and marlstones, typically rich in ammonite fauna. Strata investigated in this work comprise the lithostratigraphic units (i) Amaltheenton Fm, (ii) Posidonia Shale and (iii) Jurensismergel/Opalinuston Fm, deposited during the Pliensbachian, Toarcian and Aalenian stages. This age framework is based on various ammonite findings established in previous studies from other well sections (e.g. Arp et al., 2023; Fischer et al., 1986; van de Schootbrugge et al., 2019). The Pliensbachian Amaltheenton Fm, underlying Early Toarcian black shales is composed of marine claystones with varying carbonate contents and is generally poor in organic matter (<1 wt% TOC). In the nearby Schandelah drill core, the upper Pliensbachian Amaltheenton Fm comprises rather homogeneous light to dark-grey claystones with pyrite dispersions and frequent sideritic carbonate concretions, belonging to the *Margaritatus* ammonite zone dominated by *Amaltheus margaritatus* (van de Schootbrugge et al., 2019). Above, sediments consist of light grey bioturbated marl intercalated with limestone beds and concretions, probably belonging to the *Spinatum* ammonite zone.

Above the Pliensbachian-Toarcian boundary, a lithological transition from the organic matter-lean claystones of the Amaltheenton Fm to the laminated, organic-rich black shales of the Posidonia Shale is often observed in Germany (Meschede & Warr, 2019). Of note, particularly in the NWGB, the lowermost Toarcian (lower *tenuicostatum* zone) is often still composed of organic-lean claystones with carbonaceous concretions that resemble deposits from the upper Pliensbachian (Arp et al., 2023; Song et al., 2017; van de Schootbrugge et al., 2019). However, the *tenuicostatum* zone in the NWGB appears rather condensed compared to the SWGB, and in numerous profiles within the NWGB deposition of organic matter-rich Posidonia Shale initiates roughly

at the *tenuicostatum*/*serpentinum* zone boundary (Arp et al., 2023; van de Schootbrugge et al., 2019). The associated T-OAE, marked by a significant nCIE, typically occurs early during the *serpentinum* zone in complete profiles (Ruebsam et al., 2019; Storm et al., 2020). The Posidonia Shale consists of various facies with differing OM content and fabric types (Ajuaba et al., 2024; Arp et al., 2023; Röhl et al., 2001; van de Schootbrugge et al., 2019). Close to the base of the *bifrons* ammonite zone, a thin, carbonate-rich and fossiliferous interval with wavy lamination, known as the 'Monotis Bank', occurs, which was arguably deposited as a result of a tsunami event (Arp & Gropengießer, 2016).

Littke et al. (1991) investigated the lithostratigraphic subdivision of the Posidonia Shale in the Hils Syncline using six wells (Haddessen, Harderode, Dohnsen, Dielmissen, Wickensen, Wenzen), identifying three units (Figure S1): Unit I (marlstone with highest carbonate content), Unit II (calcareous claystone with lower than average TOC content and Hydrogen Index (HI) values) and Unit III (rather uniform calcareous claystone rich in TOC). Carbonates in these units, mainly derived from *coccolithophoridae* and *schizospheres*, appear as thin, chalky disks throughout the formation (Littke et al., 1991).

Stratigraphically, the Posidonia Shale in the NWGB extends in some localities into the Late Toarcian *Thouarsense* ammonite zone with the 'Dörnten Schiefer'. In most sections, however, and especially in the SWGB, the distal deposits of the Dörnten Schiefer are lacking and the Jurensismergel Fm unconformably superimposes Lower Toarcian black shales (Arp et al., 2021, 2023; Fantasia et al., 2019). In these cases, the transition to the Jurensismergel Fm is marked by an erosional base, condensed fossiliferous marls and conglomerates rich in fossiliferous claystone, referred to as 'Zeta-Konglomerat' and indicating a maximum regressive surface and a period of non-deposition (Arp et al., 2023). The Jurensismergel Fm consists of carbonate-bearing claystones, showing much lower TOC and HI values than the underlying Posidonia Shale Fm. The superjacent lower part of the Opalinuston Fm is composed of medium-grey, well-bedded marls with moderate TOC content, similar to the upper Jurensismergel Fm (Arp et al., 2023).

2 | MATERIALS AND METHODS

2.1 | Core description and samples

The 101 m deep Hunzen Well (BO3.0) was drilled on the southwestern flank of the Hils Syncline (Figure 1C) near Hameln, about 50 km south of Hannover, Germany (51°59′16.271″ N, 9°35′39.505″ E). Core BO3.0_HUN consists from base to top of the following lithostratigraphic formations: 28.45 m of Amaltheenton Fm, 31.02 m of Posidonia Shale Fm and about 30 m of Jurensismergel-/Opalinuston Fm. The uppermost roughly 9 m of the core can be classified as Quaternary overburden that shows signs of weathering (Figure S1). The Jurensismergel-/Opalinuston Fm are both characterised by dark grey, largely unbedded claystones and argillaceous marls, and thus are regarded as a combined lithostratigraphic unit in this work. The Posidonia Shale Fm consists of brownish-grey, horizontally laminated and bituminous argillaceous marls and, respectively, calcareous marls. Finally, the Amaltheenton Fm is composed of dark-grey claystones, often with abundant, horizontal silty laminae and a thin, argillaceous, strongly bioturbated siltstone.

Samples were taken in 1–2 cm thick segments every 0.5 to 1 m along the core, with high-resolution sampling in the Posidonia Shale at 2 cm intervals at the lithological boundaries. Samples for biostratigraphic control were taken every 1 m along the core. A total of 198 samples collected between 73 and 42 m depth were analysed using a multidisciplinary approach, including XRF, bulk rock organic carbon isotope analysis and Rock-Eval analysis (see below). These various analytical techniques were applied to obtain comprehensive geochemical data along the profile. All samples used for geochemical analysis were oven-dried (>24 h at 50°C) and crushed to a fine powder for 2 min using a disc mill (Siebtechnik B544, Germany). An aliquot of selected samples was preserved for microscopic analysis on pieces of about 3 cm^2. Furthermore, large pieces of polished core sections were prepared for detailed investigations of bedding and structural features. Polishing, however, was not possible for the Amaltheenton Fm due to its high content of clay minerals. Sample nomenclature is based on the well abbreviation and the sample depth in cm (e.g. BO3.0_4100 indicates a depth of 4100 cm (or 41 m, respectively) in well BO3.0).

2.2 | Elemental analysis

2.2.1 | X-Ray Fluorescence (XRF) spectrometry and total sulphur (TS) analysis

XRF spectrometry was performed on 48 dried and powdered samples. All samples were prepared by mixing 8 g of sediment with 2 g of Fluxana CEROX wax and pressing into aluminium ring frames. The resulting tablets were analysed using a SPECTRO XEPOS ED(P) wavelength-dispersive XRF spectrometer to determine the concentration of major and trace elements. The enrichment factor (EF) of elements was calculated relative to average shale values (Turekian & Wedepohl, 1961), using the formula

$EF = (C/Al)_{Sample}/(C/Al)_{Avg.\ Shale}$, where C is the element concentration and Al is the reference element for normalisation (Bern et al., 2019).

The total sulphur (TS) content of 20 samples, selected based on the XRF measurements, was determined using a LECO S-200 sulphur analyser. Approximately 100 ± 2 mg of dry, powdered sample material was combusted in a ceramic crucible with iron as a catalyst at 1800°C in an oxygen-rich environment. This process oxidised all sulphur compounds to sulphur dioxide (SO_2), which was then purified to remove other combustion products and detected using an infrared (IR) detector based on the Beer–Lambert law. The TS content was determined with an accuracy of ±0.01 wt% based on repeated measurements.

2.2.2 | Bulk rock organic carbon isotope analysis

A total of 104 samples was analysed for their bulk organic carbon isotope composition ($\delta^{13}C_{TOC}$) using a Flash EA 1112 elemental analyser linked to a Thermo Delta V Advantage isotope ratio mass spectrometer at BGR (Hanover, Germany). Samples were decalcified by treating 1 g of sediments with 10% HCl, then neutralised and dried at 80°C. During analysis, samples were combusted at 1020°C, resulting in the production of CO_2. The $^{13}C/^{12}C$ ratios were compared to the reference standard V-PDB (Vienna Pee Dee Belemnite) with known composition of the isotope ratio, and results were provided in conventional δ-notation as permille difference.

$$\delta^{13}C = \left[\left(\left(^{13}C/^{12}C\right)_{sample} / \left(^{13}C/^{12}C\right)_{standard}\right) - 1\right] \times 1000,$$

where $(^{13}C/^{12}C)_{sample}$ is the isotopic ratio of the sample and the $(^{13}C/^{12}C)_{standard}$ is the isotopic ratio of the reference standard V-PDB for normalisation. Analytical reproducibility was ensured by running samples and laboratory standards in replicate and was better than 0.15‰.

2.3 | Programmed temperature (Rock-Eval) pyrolysis

Rock-Eval pyrolysis was performed on 198 dried and powdered sediments using a Rock-Eval 7 instrument (Vinci Technologies, France). 20 mg of organic matter-rich samples from the Posidonia Shale Fm or 100 mg of sediment for the organic-lean Amaltheenton Fm and Jurensismergel Fm were used. Samples were placed in crucibles within an autosampler and analysed using the IFPEN (IFP Energies Nouvelles) Basic Method, involving an initial pyrolysis temperature of 300°C, holding for 3 min, and further heating to 650°C at 25°C/min (Behar et al., 2001; Grohmann et al., 2023). Hydrocarbons released during heating were transported to the flame ionisation detector (FID) by a continuous nitrogen stream. Post-pyrolysis, samples were combusted in an oxygen-rich atmosphere, with CO and CO_2 detected by an IR detector. Key parameters, including S1, S2 and S3 peaks, T_{max}, TOC and TIC, were calculated from pyrolysis curves. S2 and S3 values were used to determine the hydrogen index (HI = S2/TOC × 100) and oxygen index (OI = S3/TOC × 100), respectively. S1 and S2 peaks represent hydrocarbons volatilised at 300°C (S1) and during gradual heating to 650°C (S2), respectively. T_{max} reflects the temperature at which the maximum of hydrocarbons is formed. The S3 peak represents the CO_2 yield released up to a temperature of 390°C. Analytical accuracy was ensured by measuring laboratory standards of known composition every 10th sample.

2.4 | Organic petrography

Twelve samples, selected based on geochemical data and representing the three main lithologies, were subjected to organic petrographic analysis. Samples were cut into 1.5 × 2 cm pieces perpendicular to the bedding using a diamond circular saw. After oven drying (overnight at <30°C), samples were embedded in Teflon™ moulds (30mm inner diameter) with a two-phase epoxy resin (Araldite 2020/A and 2020/B, mass ratio 10:3) and hardened at room temperature for 12 h. Sample surfaces were ground flat and polished on Tegra Pol-21 (Struers, Germany) using diamond and quartz suspensions. Random vitrinite reflectance (VRr; %) was measured with a Zeiss Axio Imager M2m microscope fitted with a HXP 120 C illuminator, an oil immersion objective (50×/1.0 EC-Epiplan-NEOFLUAR), a Basler monochrome digital camera (1392 × 1040 px) and interference filter (546 nm), calibrated using a leuco-sapphire standard (0.592 R_0%). Reflectance was analysed using the Diskus-Fossil #10559 software from *Hilgers Technisches Büro*, adhering to Taylor et al. (1998).

3 | RESULTS

3.1 | Stratigraphic and lithologic variations; basic elemental data

The investigated sedimentary sequence comprises the three lithostratigraphic units (1) Amaltheenton Fm (2) Posidonia Shale Fm and (3) Jurensismergel-/Opalinuston Fm. Three sub-units are distinguished for the Posidonia Shale Fm based on microscopic observations and variations of inorganic geochemical parameters (Table 1 and Figure 2).

3.2 | Amaltheenton Fm

Based on the scarce biostratigraphic information obtained from the analyses of microfossils in core samples, the boundary between the lower and upper Late Pliensbachian is at about 80 m depth, corresponding to the first occurrence (FO) of benthic foraminifer *Saracenaria sublaevis* (consistent with nearby profiles investigated by Fischer et al. (1986)). Accordingly, this unit corresponds to the Lower-Upper Pliensbachian. This argillaceous sequence contains siderite ($FeCO_3$) concretions as indicated by locally elevated TIC values in two samples reaching 3.51 and 8.04 wt% (mean 5.78 ± 3.20 wt%; at 88 and 77 m depth). Assuming that this TIC entirely represents siderite ($FeCO_3$), the siderite content can be calculated by multiplying by 9.58. Thus, siderite contents of 33.6 and 77.0 wt% are estimated for the concretions (Figure 2). This interval shows a low to moderate TOC content, ranging from 0.35 to 1.10 wt% (mean 0.61 ± 0.36 wt%). The Amaltheenton Fm exhibits low TIC values, except for the siderite concretions ranging from 0.15 to 8.04 wt% (mean 0.91 ± 1.65 wt%). TS values scatter widely from 0.08 to 8.51 wt% (mean 1.97 ± 3.23 wt%). Relatively high percentages of terrigenous macerals (vitrinite, resedimented vitrinite, inertinite; exceeding 70% by volume) are noted within the Amaltheenton Fm, while liptinites derived from aqueous organic matter are rare (Figure 2). Furthermore, the Amaltheenton Fm is characterised by high abundances of Al_2O_3 ranging from 20.54 to 25.23 wt% (mean 22.07 ± 1.73 wt%), Fe_2O_3 varying from 4.54 wt% to 9.05 wt% (mean 6.72 ± 1.67 wt%) and SiO_2 ranging from 46.49 to 56.86 wt% (mean 51.36 ± 3.73 wt%) and an elevated Ag content, with an enrichment factor (EF) exceeding 5 (Figure 3; Table 1; Table S1).

The uppermost part of the Amaltheenton Fm (77–72.55 m) is lithologically similar, but geochemically slightly different. It is characterised by lower TIC values ranging from 0.13 to 6.88 wt% (mean 1.22 ± 2.51 wt%). TOC values

TABLE 1 Results of elemental analysis, including total organic carbon (TOC), total inorganic carbon (TIC), total sulphur (TS) content and XRF data of major element oxides and stable carbon isotopes of organic matter ($\delta^{13}C_{TOC}$).

Formation	TOC [wt%]	TIC [wt%]	TS [wt%]	Al_2O_3 [wt%]	SiO_2 [wt%]	Fe_2O_3 [wt%]	CaO [wt%]	$\delta^{13}C_{TOC}$ [‰ V-PDB]
Jur/Opa Fm								
Min	1.06	0.37	1.31	19.52	42.93	3.54	4.82	−27.90
Max	2.55	1.69	1.82	20.37	46.42	5.93	6.42	−26.10
Av	1.75	0.89	1.57	19.86	44.52	4.62	5.51	−27.41
Posi. Unit III								
Min	7.39	1.77	2.86	8.03	24.80	2.71	19.57	−28.60
Max	12.95	5.37	8.42	9.61	29.03	14.74	22.51	−27.90
Av	10.16	3.97	5.20	8.83	26.68	5.84	21.12	−28.21
Posi. Unit II								
Min	0.75	2.46	3.82	0.37	2.98	2.28	17.68	−28.60
Max	10.20	10.53	4.41	12.94	34.01	24.18	38.00	−28.00
Av	7.13	4.96	4.08	8.13	22.39	7.06	24.48	−28.43
Posi. Unit I								
Min	2.02	2.48	2.46	1.68	5.36	2.84	17.46	−29.00
Max	16.01	10.81	4.34	11.85	31.23	5.75	41.36	−26.30
Av	9.10	6.71	3.69	5.61	16.13	3.90	29.58	−27.42
Upper AMA								
Min	0.62	0.13	2.99	20.84	54.31	3.91	0.58	−27.60
Max	2.78	6.88	3.61	24.07	60.26	6.55	1.43	−25.60
Av	0.90	1.22	3.30	22.48	57.65	5.16	1.03	−26.04
Amaltheenton Fm								
Min	0.35	0.15	0.08	20.54	46.49	4.54	0.92	−26.70
Max	1.10	8.04	8.51	25.23	56.86	9.05	1.74	−25.50
Av	0.81	0.91	1.97	22.07	51.36	6.72	1.32	−26.05

Note: For each subunit, the minimum (Min), maximum (Max) and average (Av) value is given. Upper AMA, uppermost Amaltheenton Fm.

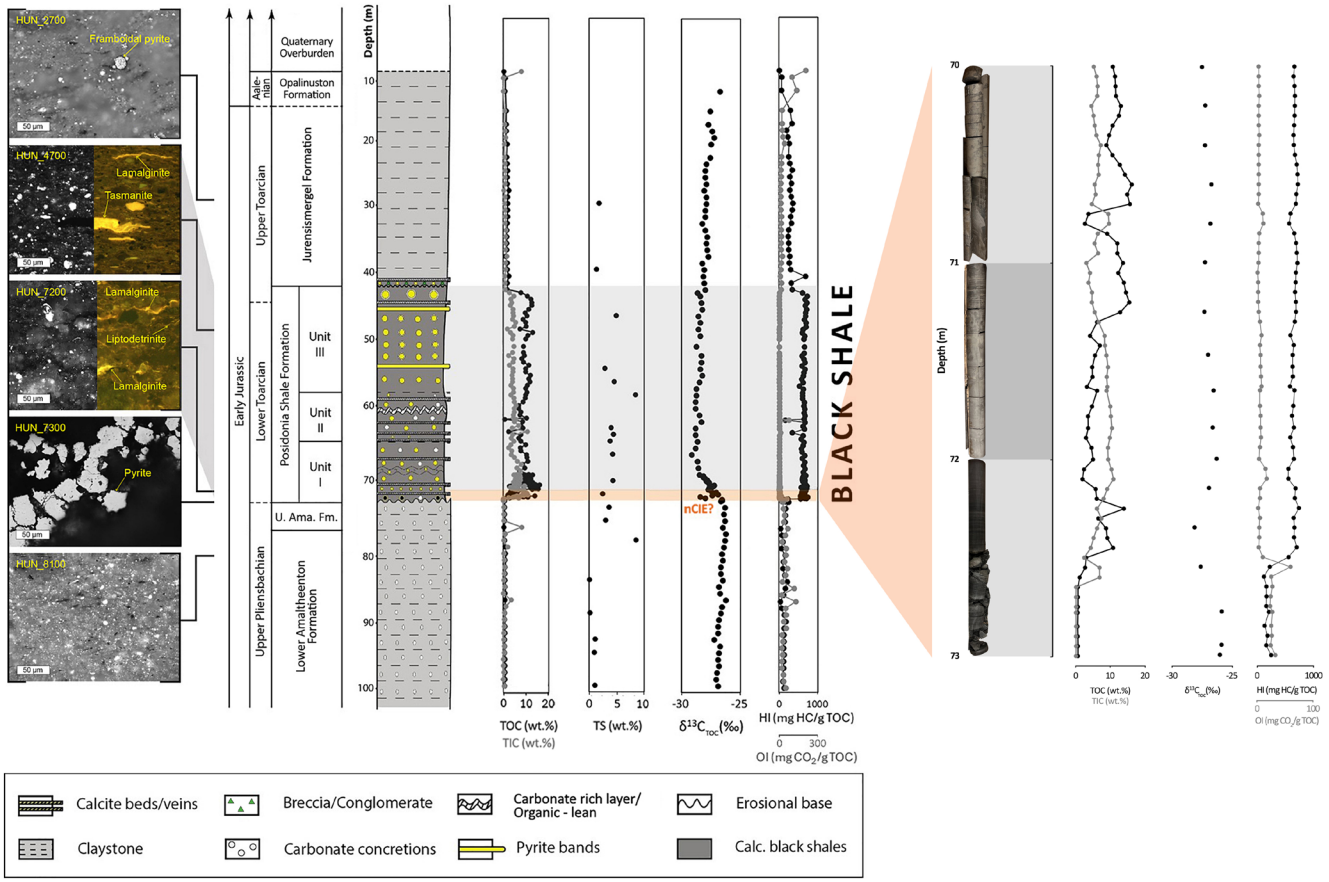

FIGURE 2 Lithostratigraphic overview of the Hunzen sedimentary succession with representative photomicrographs of sedimentary units (macerals in incident light). Organic and inorganic parameters are plotted downcore. Total organic carbon (TOC) and total inorganic carbon (TIC) content, total sulphur (TS) content, bulk organic carbon isotopes ($\delta^{13}C_{TOC}$), hydrogen index (HI) and oxygen index (OI) values. A detailed view of the downcore plot of organic and inorganic parameters in the transition zone (73–70 m) is shown, highlighting variations in TOC, TIC content, $\delta^{13}C_{TOC}$, HI and OI. Note that the negative carbon isotope excursion (nCIE) marked in Unit I probably represents only the rising limb of the excursion, as the plateau and recovery phases are possibly missing due to stratigraphic condensation or a hiatus (see Section 4.2 and 4.3 for details).

range from 0.62 to 2.78 wt% (mean 0.90 ± 0.58 wt%), while TS values vary from 2.99 to 3.61 wt% (mean 3.3 ± 0.44 wt%) (Figure 2). Al_2O_3 contents are high, ranging from 20.84 to 24.07 wt% (mean 22.48 ± 1.23 wt%), while Fe_2O_3 values vary from 3.91 to 6.55 wt% (mean 5.16 ± 0.96 wt%) and SiO_2 from 54.31 to 60.26 wt% (mean 57.65 ± 2.55 wt%), that is, the interval is enriched in Fe and Si relative to the Amaltheenton Fm below 77 m (Table 1; Table S1). Furthermore, Hg levels are high (Figure 3). Iron-oxide staining patterns in the uppermost layer suggest oxidation of former pyrite aggregates.

3.3 | Posidonia Shale Fm

The Posidonia Shale Fm (72.55 to 41.50 m) comprises three lithological sub-zones (Units I, II, III). It is composed of dark, brownish-grey and bituminous argillaceous and calcareous marls with some carbonate beds. Overall, these 'black shales' are well-laminated and rich in macroscopic pyrite and macrofossils such as ammonites and belemnites. Lamination results from alternating carbonate-rich light-coloured and clay-rich dark-coloured horizons as described in detail in Littke et al. (1991), indicating deposition in a quiet, undisturbed and anoxic environment below wave base, where bottom currents and bioturbation were minimal. The studied core interval includes the Lower Toarcian CIE and OAE (Röhl et al., 2001; Röhl & Schmid-Röhl, 2005; Ruebsam et al., 2024). Geochemically, the formation is characterised by high TOC, TIC and TS values (Figure 2, Table 1). Pyrite occurs as intercalated bands, concretions, finely disseminated small crystals and framboids, with TS contents ranging from 2.46 to 8.42 wt%, and slight variations among sub-units: Unit I ranging from 2.46 to 4.34 wt% (mean 3.69 ± 1.07 wt%) has slightly lower TS content than Units II, ranging from 3.82 to 4.41 wt% (mean 4.08 ± 0.30 wt%) and III ranging from 2.86 to 8.42 wt% (mean 5.20 ± 2.33 wt%; Table 1).

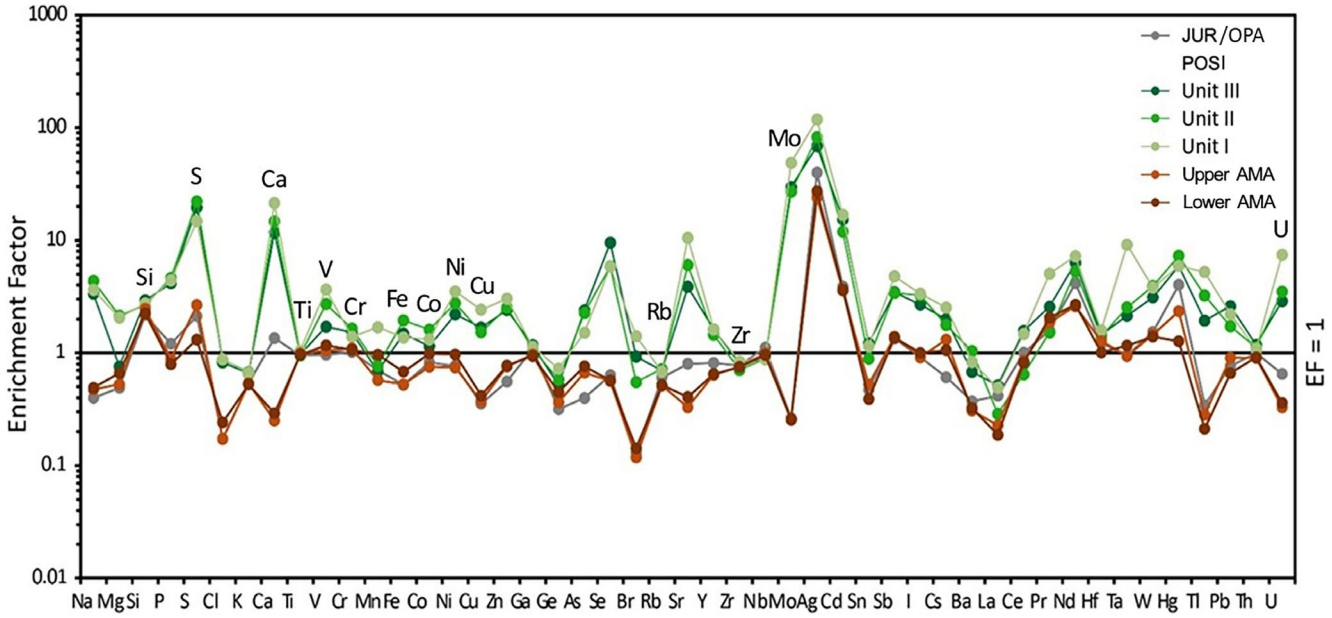

FIGURE 3 Trace element enrichment (EF >1) and depletion (EF <1). EF is given as average values for the studied stratigraphic intervals: JUR, Jurensismergel Fm; POSI, Posidonia Shale Fm; Upper AMA, uppermost Amaltheenton Fm; Lower AMA, Lower Amaltheenton Fm.

Unit I is enriched in TOC except for some carbonate beds ranging from 2.02 to 16.01 wt% (mean 9.10 ± 3.54 wt%) and TIC ranging from 2.48 to 10.81 wt% (mean 6.71 ± 1.85 wt%). Unit II maintains relatively high TOC content, though slightly lower than in Units I and III, ranging from 0.75 to 10.20 wt% (mean 7.13 ± 2.48 wt%) and TIC content ranging from 2.46 to 10.53 wt% (mean 4.96 ± 1.86 wt%), while Unit III shows only moderate TIC ranging from 1.77 to 5.37 wt% (mean 3.97 ± 0.81 wt%) and the highest TOC ranging from 7.39 to 12.95 wt% (mean 10.16 ± 1.39 wt%) (Figure 2, Table 1). An exceptional carbonate-rich layer at 60.65 m in Unit II, probably equivalent to the 'Oberer Stein' horizon, shows, in comparison with other parts of Unit II, lower TOC (0.75 wt%) and higher TIC (5.69 wt%) contents (Table 1, Table S2), consistent with observations by Röhl et al. (2001). White carbonate concretions and vein fillings were observed macroscopically (Figure 4A).

The maceral composition of the Toarcian black shales is dominated by liptinite, mainly alginite (telalginite derived from Tasmanites and lamalginite) derived from primary marine production, as well as liptodetrinite and bituminite. Vitrinite and inertinite as well as sporinite as terrigenous macerals are rare (Figure 2), in agreement with observations from the SWGB (Ajuaba et al., 2022, 2024). While primary vitrinite (autochthonous) is rare, resedimented vitrinites showing VRr values of 0.9% or higher are more abundant, indicating detrital material enriched in organic matter. Additionally, framboidal pyrite is much more abundant in the Posidonia Shale Fm compared to the overlying and underlying claystones. The Posidonia Shale Fm exhibits lower Fe_2O_3, SiO_2 and Al_2O_3 contents and higher CaO compared to the underlying OM-lean claystone. Al_2O_3 and SiO_2 increase progressively towards the uppermost sub-zone, while CaO decreases from Unit I towards Unit III. Unit II is enriched in Fe_2O_3 relative to Unit I, with values ranging from 2.28 to 24.18 wt% (mean 7.06 ± 7.69 wt%). Unit I ranges from 2.84 to 5.75 wt% (mean 3.90 ± 0.78 wt%) and Unit III varies from 2.71 to 14.74 wt% (mean 5.84 ± 4.15 wt%) (Table 1). The trace elements Ni, Cu, Zn, Ag, Cd, Mo, U and Sr are enriched in the Posidonia Shale Fm, with Ag and Mo showing high enrichment (EF >10) and Se, Sr, Cd and U displaying only a moderate enrichment (EF >5). Elemental concentrations, particularly U, Mo, Cu, Sr and V, are higher in Unit I and decrease to the uppermost layers (Figure 3).

3.4 | Jurensismergel-/Opalinuston Fm

The Jurensismergel Fm is lithologically identical with the overlying Opalinuston Fm; in the following it is called Jurensismergel-/Opalinuston Fm (41.5 to about 9 m). It is marked by moderate TOC values ranging from 1.06 to 2.55 wt% (mean 1.75 ± 0.34%) and TIC contents ranging from 0.37 to 1.69 wt% (mean 0.89 ± 0.25 wt%). Furthermore, the formation shows moderate TS contents, higher CaO abundances and lower concentrations of Al_2O_3, SiO_2 and Fe_2O_3 compared to the Amaltheenton Fm with values of 19.52 to 20.37 wt% (mean

FIGURE 4 Core photos: (A) One-meter core section (63 to 64 m) highlighting white carbonate concretions and vein fillings. Note the typical fine lamination of the Posidonia Shale Fm; (B) Transition zone between the Upper Pliensbachian Amaltheenton Fm (bottom) and Posidonia Shale Fm (depth ~72.50 m), marked by a 15 cm transitional interval from dark-grey claystone to laminated, pyrite-rich black shale and (C) Transition zone between the Posidonia Shale Fm (bottom) and Upper Toarcian Jurensismergel Fm (depth ~41.48 m), marked by an erosional contact.

19.86 ± 0.45 wt%), 42.93 to 46.42 wt% (44.52 ± 1.77 wt%) and 3.54 to 5.93 wt% (mean 4.62 ± 1.22 wt%), respectively. The trace element patterns are similar to those in the Amaltheenton Fm. The uppermost 2–3 m below Quaternary overburden show indications of weathering and were not investigated.

4 | DISCUSSION

4.1 | Contact relationships

The transition from dark-grey claystones of the Amaltheenton Fm to laminated black shales rich in

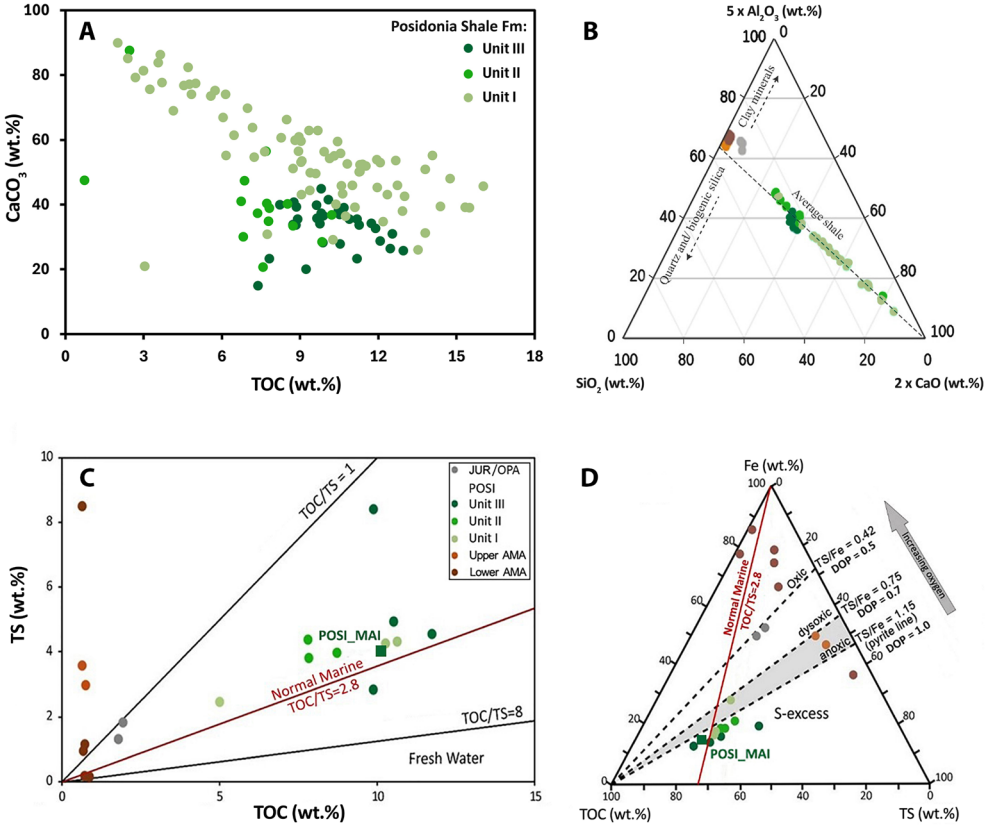

FIGURE 5 (A) Cross-plot of $CaCO_3$ and TOC for the Posidonia Shale Fm. Note a higher sampling frequency in Unit I compared to Units II and III; (B) Ternary diagram of Al_2O_3-CaO-SiO_2 relative concentrations (Wu et al., 2024) in the Hunzen Well. Average shale values are shown for comparison (Wedepohl, 1971, 1991); (C) TOC versus TS plot with trendline for normal marine conditions (modified after Berner & Raiswell, 1984); (D) Ternary plot of the relative abundances of TOC-TS-Fe with interpretative areas for S-excess, anoxic, dysoxic and oxic conditions (modified after Dean & Arthur, 1989); see text for explanation.

pyrite occurs over an interval of about 15 cm at ~72.50 m depth (Figure 4B). The conglomeratic layer in between comprises belemnites and fragments of shells, indicative of an erosional or non-depositional surface. Similar unconformities at the base of the Posidonia Shale Fm, biostratigraphically comprising roughly the *tenuicostatum* zone, were reported not only from southern Germany (Arp et al., 2021) but also in several other profiles in the NWGB, including Schandelah (Ruebsam et al., 2024; van de Schootbrugge et al., 2019), Hondelage (Marten et al., 2024; Mutterlose et al., 2022) and Core A (Celestino et al., 2024). However, numerous other Lower Jurassic profiles within the Lower Saxony Basin, including those discussed by Arp et al. (2023) suggest continuous sedimentation across the Pliensbachian–Toarcian boundary, indicating spatial variability in depositional continuity. Below the unconformity in Core BO3.0_HUN, the uppermost Amaltheenton Fm is characterised by the presence of soft clay with concentric iron-oxide staining patterns surrounding former or still existing pyrite aggregates (Figure 4B). This observation is indicative of the effects of oxidation. The transition zone at the base of the Posidonia Shale Fm is characterised by upwards increasing TOC and HI values, roughly between 2 and 3 wt% and 100 and 200 mg HC/g TOC, respectively (Figure 2). Carbonate contents and OI values are high in this interval. The black shale contains mm-thin, whitish stripes of carbonate in this lowermost part. Within the lowermost 50 cm of the 31.02 m thick Posidonia Shale Fm, a n-CIE is observed together with a high carbonate content (Figure 2). Above about 72.50 m depth, HI values and TOC contents are constantly high, with the exception of some carbonate-rich layers within Units I and II where TOC values are lower than average. Generally, TOC and carbonate content are negatively correlated within the Posidonia Shale Fm (Figures 2 and 5A).

The transition from the uppermost part of the Posidonia Shale Fm (Unit III) to the Jurensismergel Fm is marked by a cm-thick breccia/conglomerate (Lias ʒ conglomerate) with accumulations of reworked and often bioeroded ammonites and belemnites (Figure 4C). This conglomerate is indicative of a widespread stratigraphic gap at the transition between the Lower and Upper Toarcian and occurs in sections within both northern and southern Germany (Arp et al., 2021, 2023).

4.2 | General geochemical trends

The $\delta^{13}C_{TOC}$ values fluctuate between −25.5‰ and −29.0‰, with a nCIE at the base of the black shale deposit (Figure 2; Table S1). $\delta^{13}C_{TOC}$ values are 'heavier' (less negative) in the Amaltheenton Fm than in the Posidonia Shale Fm, with highest values reaching −25.5‰ to −26.7‰ (avg. −26.1‰). A positive CIE at 88 m may align with the Upper Pliensbachian *Margaritatus* zone of well Schandelah-1 (CJ8) (Röhl et al., 2001; van de Schootbrugge et al., 2019). Furthermore, an interval characterised by a siderite concretion (77 m) exhibits less negative isotopic values (−25.8‰), which is probably due to diagenetic carbonate precipitation and incorporation of isotopically heavy CO_2 into organic matter (Röhl et al., 2001). Within the OM-lean interval between 100 and 73 m, there is a trend towards slightly less negative isotope values (Figure 2). Samples within the T-CIE of Unit I (72.50–65.44 m) of the Posidonia Shale Fm exhibit more negative $\delta^{13}C_{TOC}$ values, with a range of −26.3‰ to −29.0‰ (avg. −27.4‰). This interval is characterised by distinct laminations. However, the magnitude of the nCIE in this section is less pronounced compared to the 1.4 m thick interval at well Schandelah-1 (CJ9), which records $\delta^{13}C_{TOC}$ values as low as −33.2‰, possibly due to variations in OM sources associated with the T-OAE (van de Schootbrugge et al., 2019) or missing sections in the Hunzen well. As similar $\delta^{13}C_{TOC}$ values below −30‰ have also been reported from Hondelage, Barth, KSS5 and Core A (Celestino et al., 2024; Marten et al., 2024; Ruebsam et al., 2024), the full nCIE is probably indeed missing in the Hunzen well and only the rising limb of the $\delta^{13}C_{TOC}$ excursion is preserved.

Above this section, sediments follow which are characterised by a weak positive $\delta^{13}C_{TOC}$ excursion (Figure 2; between 72.0 and 71.7 m) corresponding to the post-nCIE observed in van de Schootbrugge et al. (2019), possibly driven by enhanced organic carbon burial. Above the nCIE, $\delta^{13}C_{TOC}$ values decrease continuously towards the top of Unit I (Figure 2). Units II and III show stable $\delta^{13}C_{TOC}$ values, averaging at −28.3‰ (ranging from −28.6‰ to −27.9‰) and slightly increasing towards the top of the Posidonia Shale Fm (Figure 2), indicating that the dissolved carbon reservoir became progressively isotopically heavier. The transition to the Jurensismergel Fm is marked by a ~1‰ increase in $\delta^{13}C_{TOC}$ values and a trend to slightly heavier isotope values towards the core top.

The thermal maturity, origin, type and preservation of OM in the studied well section were characterised by Rock-Eval pyrolysis, revealing significant variations across lithologies (Figures 2 and 6). The Hunzen well section shows high HI values for the Posidonia Shale Fm (avg. 638 mg HC/g TOC) and relatively low T_{max} values (avg. ~442°C), indicative of an early mature petroleum source rock (Stock et al., 2017). The covariance of HI and T_{max} values along with low OI values (avg. 5 mg CO_2/g TOC) (Figure 6) supports this finding, which is consistent with data from Fang et al. (2019) for the Posidonia Shale at different maturity levels. Vitrinite reflectance values of 0.70% align with an early stage of petroleum formation and are in agreement with the general trend observed along the southern limb of the Hils Syncline, showing increased thermal maturities from SE to NW (Figure 1C;

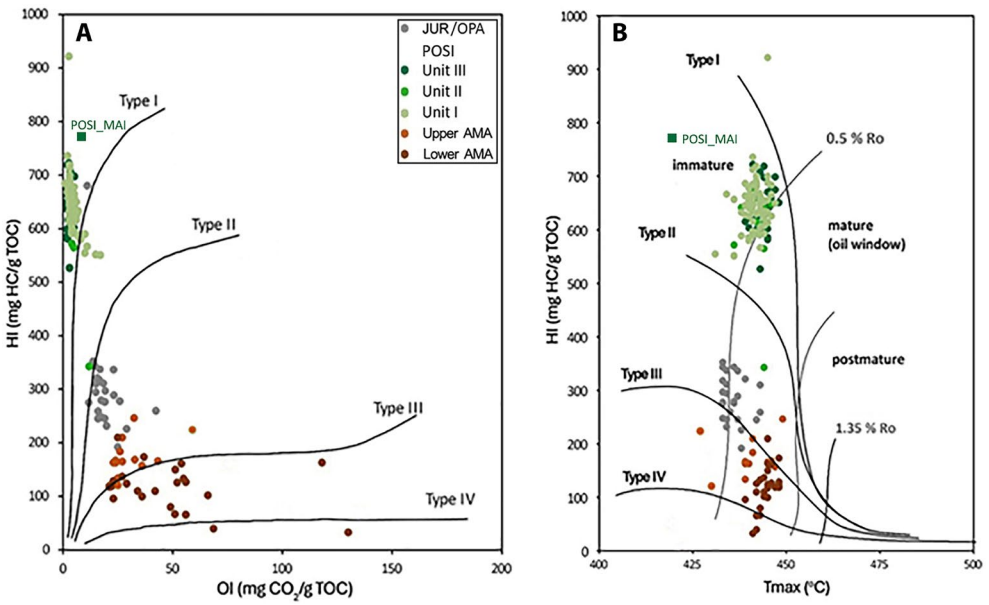

FIGURE 6 Rock-Eval parameters: (A) relationship between HI and OI values and (B) between HI and T_{max} values. Note that the vitrinite reflectance value for all units in the Hunzen Well is 0.70%, and 0.50% for the Mainzholzen Well.

Burnaz et al., 2024; Fang et al., 2019; Littke et al., 1991). Based on its thickness (about 30 m), TOC content (about 10 wt%) and HI values (about 700 mg HC/g TOC at immature stage), the Posidonia Shale in northern Germany is classified as an excellent petroleum source rock (Song et al., 2015; Stock et al., 2017). In borehole Mainzholzen (MAI), drilled just 15 km to the south-east of borehole Hunzen, organic matter is thermally immature. Compared to Hunzen, MAI samples exhibit slightly higher HI and OI values (Figure 6A). The results of the MAI samples provide the full petroleum generation potential of the Posidonia Shale, while at Hunzen, a small part has already been consumed upon maturation.

The Amaltheenton Fm is characterised by low-moderate HI (avg. 117 mg HC/g TOC) and moderate OI (avg. 47 mg CO_2/g TOC) values, indicating a kerogen type III and low to moderate potential for hydrocarbon generation. Siderite-rich layers at 77 m have even lower HI (40 mg HC/g TOC) but higher OI (69 mg CO_2/g TOC) values, indicating kerogen degradation during early diagenetic siderite growth and/or CO_2 generation during siderite decomposition at pyrolysis temperatures below 390°C. Siderite is known to be less stable under pyrolysis conditions than calcite and dolomite (Pillot et al., 2014). Consequently, the pyrolysis of siderite results in a kerogen type IV signature (Lis et al., 2022; Plet et al., 2016). Within this well section, the Posidonia Shale Fm exhibits the highest HI values (624 mg HC/g TOC) (Figure 6) and can be regarded as an excellent petroleum source rock. OM enrichment varies across sub-zones, with Units I (9.10 wt%) and III (10.16 wt%) showing higher average TOC values than Unit II (7.13 wt%) which corroborates with the TS, Mo and U enrichment pattern (Table 1, Figure 3). High HI values (638 mg HC/g TOC) suggest well-preserved marine OM derived mainly from phytoplankton (kerogen types I and II), while average OI values (5 mg CO_2/g TOC) are lower than in the adjacent claystone layers. Units I to III show average HI values of 648, 582 and 642mg HC/g TOC, respectively, whilst average OI values are 4, 9 and 3 mg CO_2/g TOC, respectively.

The transition to the Jurensismergel Fm is marked by a sharp decline in TOC content to 1.75 wt% (Figure 2). In comparison to the underlying Amaltheenton Fm, however, the Jurensismergel Fm exhibits higher TOC values. HI values (average 300 mg HC/g TOC; Figure 2; Table S2) are generally moderate to high, while OI values are low to moderate (average 19 mg CO_2/g TOC), indicative of the deposition of kerogen type II.

4.3 | Depositional system

The sedimentary sequence of the Hunzen well is interpreted based on lithological and geochemical variations and compared with the results from previously studied profiles in northern and southern Germany (Röhl et al., 2001; Röhl & Schmid-Röhl, 2005; Zimmermann et al., 2015).

4.3.1 | Amaltheenton Fm

Redox conditions in sedimentary environments can be inferred from the relative proportion of TOC and TS (Berner, 1984; Röhl et al., 2001; Thibault et al., 2018). In anoxic depositional environments, sulphate-reducing bacteria oxidise organic compounds while reducing sulfate (SO_4^{-2}) to hydrogen sulfide (HS^-), bicarbonate ions (HCO_3^-) and residual non-metabolisable OM, leading ultimately to the formation of framboidal pyrite in the presence of reactive iron during early diagenesis in sediments or even within the water column (Wilkin et al., 1996). However, the interpretation should be made with caution, because influences such as for example, thermal maturation lead to relative shifts in TOC/TS ratios (Hart & Hofmann, 2022).

In the Amaltheenton Fm, both TOC and TS values are low with only a few exceptions (Figure 5C). This suggests minor sulphate-reducing bacterial activity and aerobic OM degradation. The higher TS content (and thus lower TOC/TS ratios; Figure 5C) in the uppermost Amaltheenton Fm indicates either more reducing conditions close to the transition to the black shale unit or, more probably, short-distance downward transport of HS^- from the overlying sapropels. It is reasonable to assume that pore water below the newly deposited sapropels turned from oxic to anoxic, promoting biological sulphate reduction and pyrite formation.

The TOC-TS-Fe relationship (Figure 5D) points to oxic depositional conditions for the Amaltheenton Fm. The TS/Fe stoichiometric ratio ('pyrite line' ~1.15) reveals varying degrees of pyritisation (DOP; Berner et al., 2013; Dean & Arthur, 1989; McArthur et al., 2008), with DOP values indicating oxic conditions in the shallow marine sediments of the Amaltheenton Fm, but progressing oxygen depletion of bottom waters in sediments below the black shale. The formation of diagenetic pyrite within the claystone (e.g. BO3.0_7300; Figure 2) aligns with anoxic pore water conditions during diagenesis, as corroborated by the formation of a greater pyrite fraction within or on the sheet silicate layers (Canfield et al., 1992). Excess Fe relative to S suggests the presence of non-pyrite Fe forms, probably the reactive Fe fraction in detrital minerals and siderite. This is supported by abundant siderite concretions in the Amaltheenton Fm (e.g. BO3.0_7700) formed during early burial under neutral to alkaline pH, low oxygen and low palaeosalinity (Burnaz et al., 2024; Curtis et al., 1986; Raiswell & Fisher, 2000).

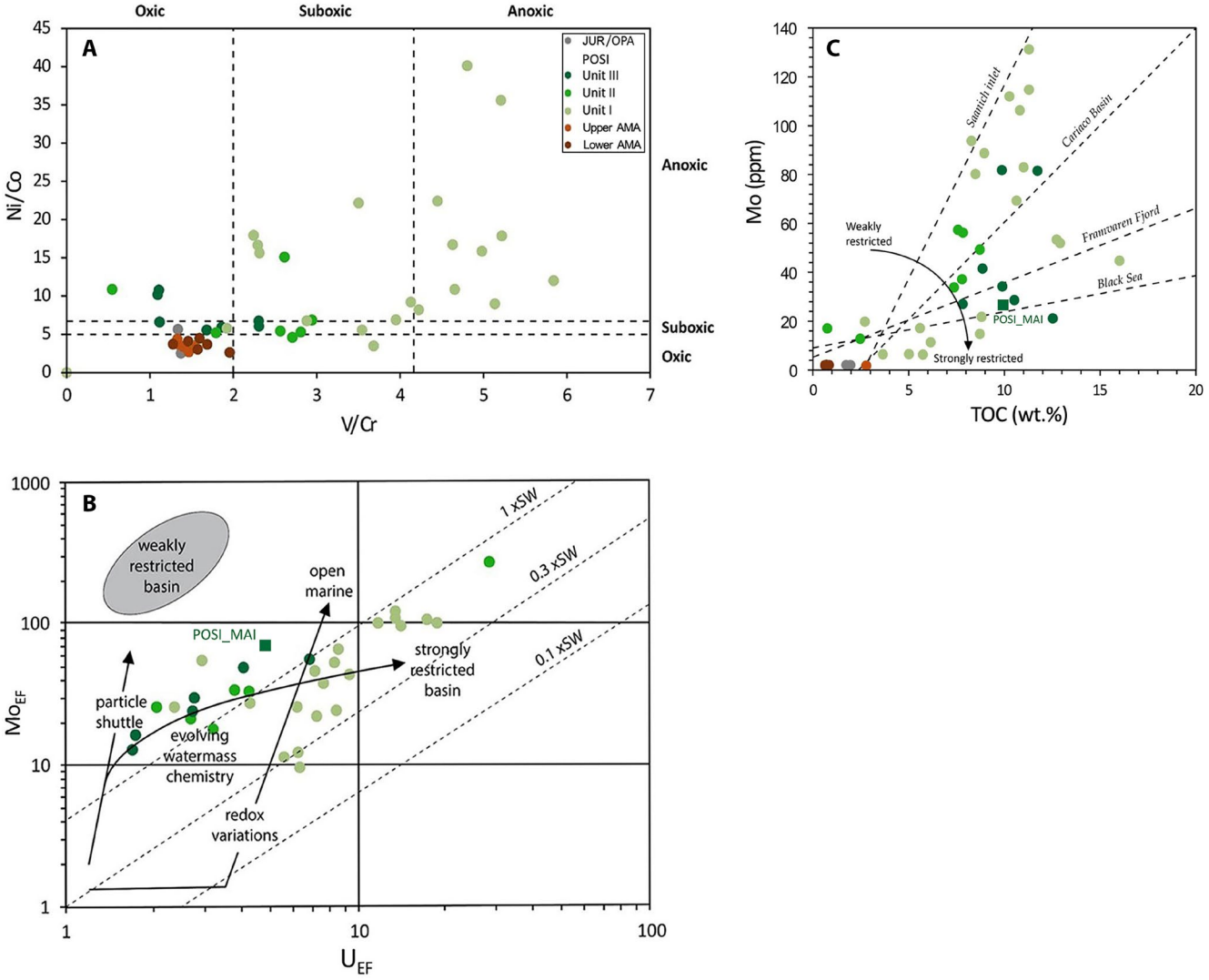

FIGURE 7 (A) Ni/Co versus V/Cr ratios with trendline indicating variations in redox conditions (modified after Togunwa & Abdullah, 2017); (B) enrichment of Mo (Mo_{EF}) versus U (U_{EF}) with trendlines related to variations in redox conditions, basin restriction and particulate shuttle. Dotted lines represent the Mo/U ratios in sea water (SW) (modified after Algeo & Tribovillard, 2009); (C) Mo concentration versus TOC values, indicative for the degree of basin restriction and deepwater age (modified after Rowe et al., 2008).

Redox-sensitive trace metals are more soluble under oxidising conditions and less soluble in oxygen-depleted environments. While Cu, Ni, Cr and Co are indicative of weak euxinic conditions, U, V, Zn and Mo suggest stronger euxinia (Algeo & Maynard, 2008). The low Ni/Co and V/Cr ratios point to oxic bottom and pore water conditions (Tribovillard et al., 2006) during the deposition of the Amaltheenton Fm (Figure 7A).

Continental weathering controls the rate of terrigenous runoff into marine basins and has been studied using elemental proxies such as Si/Al, Zr/Rb and Ti/Al, providing insights into sedimentary dynamics and depositional environments (Xu et al., 2018). High abundances of Ti, Zr and Si indicate significant detrital input (Fantasia et al., 2019), although there are also marine sources of Si (e.g. siliceous sponges). Si and Zr are often associated with coarser quartz and zircon, while Al and Rb correlate with finer clay minerals. Ti, found in heavy minerals such as ilmenite and rutile, reflects gravitational fractionation during transport processes. Therefore, Si/Al and Zr/Rb ratios indicate grain-size variations, while the Ti/Al ratio offers insights into transport distances of detrital material (Kemp et al., 2005; Them, Gill, Selby, et al., 2017; Xu et al., 2018).

In the Amaltheenton Fm, Si/Al, Ti/Al and Zr/Rb ratios are rather constant (Figure 8) indicating the deposition of claystone distant from land. High terrigenous input is evident from elevated Fe_2O_3 abundances (avg. 6.72 wt%; Table 1) and low Ca/(Ca + Fe) ratios (Figure 8). Ga primarily originates from feldspathic silicate and quartzose rocks and exhibits a strong affinity for clay mineral adsorption. Marine sediments typically contain <15 ppm Ga and thus have a

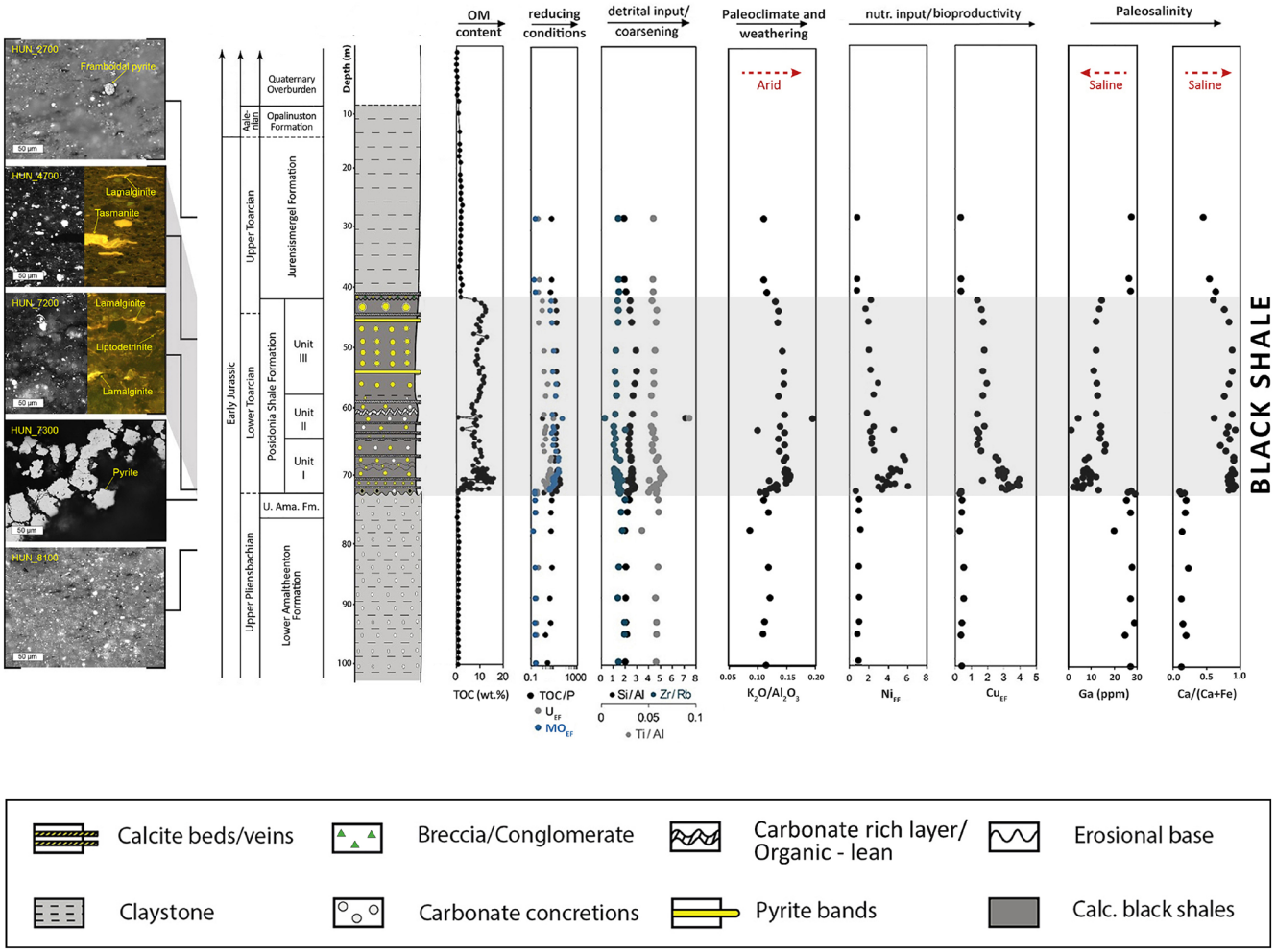

FIGURE 8 Variations of palaeodepositional conditions: Organic matter content based on TOC values; high values indicate anoxic or suboxic bottom water; reducing bottom water conditions based on TOC/P ratios and Mo_{EF} as well as U_{EF} values (see Figure 7 and text); detrital input/coarsening based on Si/Al, Zr/Rb and Ti/Al ratios; weathering intensity/humidity based on K/Al ratios; nutrient input and bioproductivity based on Ni_{EF} as well as Cu_{EF} values; palaeosalinity based on Ga concentrations and Ca/Fe ratios. See also the following figures and text for explanation.

lower concentration than freshwater sediments. According to the high Ga concentrations in the Amaltheenton Fm, rather low salinity and possibly brackish water conditions are indicated. The Ga concentration displays an inverse relationship with the Ca/(Ca+Fe) ratio (Figure 8) with both indicators corroborating evidence of strong terrigenous contributions to the Amaltheenton Fm. K_2O/Al_2O_3 ratios are generally lower than in the Toarcian section, indicating strong weathering, probably in a warm and humid climate. This contrasts with the expected increase in weathering intensity during the T-OAE associated with a warm and humid climate (Merkel & Munnecke, 2023; Ruebsam et al., 2019; Schwark & Ruebsam, 2024; Suan et al., 2011). However, the recent work by Jarvis et al. (2024) also shows that an increase in phyllosilicate proxies, such as K/Al at the Pliensbachian-Toarcian boundary, occurred alongside a facies shift towards finer-grained mudstones and TOC enrichment, reflecting reduced sand/silt input and increased adsorption of organic matter to clay minerals. Hence, aside from climate, factors such as sediment provenance, mineral sorting, or recycling may influence the lower K_2O/Al_2O_3 signal of Amaltheenton Fm of well Hunzen. Alternatively, regional differences in climate or weathering intensity may have produced enhanced kaolinite formation and leaching in the Pliensbachian catchments feeding the NWGB. In any case, the very low K/Al ratios of the Amaltheenton Fm must be related to strong weathering.

The relative contribution of SiO_2-Al_2O_3-CaO (Figure 5B) highlights the interplay between quartz and/or biogenic silica, calcium carbonate mainly of biogenic origin and clay components, offering insights into sediment provenances and depositional environments (Rachold & Brumsack, 2001). The clustering of the Amaltheenton Fm close to the Al_2O_3 corner indicates the dominance of clay minerals, which are typically derived from strong chemical weathering of continental rocks and reflect high

terrigenous input into marine environments (Rachold & Brumsack, 2001). The lack of deviation towards the SiO_2 apex further suggests that biogenic silica is not present.

Sedimentary OM in coastal-marine basins typically originates from terrigenous and marine sources. TOC-$\delta^{13}C_{TOC}$ patterns (Figure 9A) reflect both global carbon burial and isotopic variations, while the $\delta^{13}C_{TOC}$-HI correlation (Figure 9B) can be used to differentiate between productivity-controlled and preservation-controlled environments (Dean & Gardner, 1998; Lehmann et al., 2002; Röhl & Schmid-Röhl, 2005).

The Amaltheenton Fm exhibits a positive upward $\delta^{13}C_{TOC}$ trend (Figure 2), indicating increased terrigenous clastic OM input as also evidenced by a strong $\delta^{13}C_{TOC}$ and HI correlation as well as overall low HI and enriched $\delta^{13}C_{TOC}$ values. A slight upward-increasing HI trend points to better preservation conditions than in the section below, aligning with a divergent $\delta^{13}C_{TOC}$-HI relationship.

Low HI and TOC values together with high OI values (Figure 2) of the Amaltheenton Fm are indicative of poor OM preservation and a high OM decomposition rate under permanently oxic conditions. The OM in these marine sediments is classified as type III kerogen, which is primarily terrigenous in origin (Figure 6). This is in accordance with the relatively high sedimentary $\delta^{13}C_{TOC}$ values (Figure 9B). The Amaltheenton Fm shows rather uniform HI and OI values with only little variation (Figure 2), suggesting relatively stable OM sources and redox conditions. Some intervals (e.g. at 88 and 77 m depth) with slightly higher HI and lower OI values correspond to carbonate-rich layers or siderite concretions. Slightly higher HI and lower OI values in the uppermost 4 m of the Amaltheenton Fm imply either a shift of the OM sources towards a higher marine contribution or better preservation conditions under oxygen-depleted conditions, in accordance with observations on recent marine sediments (Lückge et al., 1999; Figure 2, see also Figure 9B). The data thus suggest that the Amaltheenton Fm represents deposition in a shallow marine and predominantly fully oxygenated environment. Under a humid climate, much silicate was transported to the sea due to increased runoff. In the clay-rich, fine-grained sedimentary rocks, almost no marine organic matter is preserved, but some terrigenous phytoclasts. During the Upper Pliensbachian, the epicontinental sea was composed of well-mixed water with periodically deep-reaching waves that were probably triggered by mega-monsoonal climatic conditions (Parrish, 1993; Röhl & Schmid-Röhl, 2005). This situation may have led to seasonally controlled warm freshwater inflow into the sea, together with abundant clay minerals and associated elements such as Fe, Al, Ti (Figures 3 and 8). The main suppliers of terrigenous material were the Fennoscandian High in the north-east and the Bohemian Landmass in the south-east, but possibly also the Rhenish Massif in the southwest together with some smaller islands (Figure 1). Interestingly, siderite concretions are common and partly several centimetres or even decimetres thick. These concretions formed at an early diagenetic state under slightly reducing conditions in the pore water.

The Upper Pliensbachian *Margaritatus* ammonite zone is assumed to be associated with a long-term sea level rise and rather warm and humid climatic conditions, supported by abundant benthic organisms (van de Schootbrugge et al., 2019). Arguably, these conditions may correspond to the 101–88 m interval in the Hunzen well, associated with a slight increase in detrital influx and a gradual decrease in $\delta^{13}C_{TOC}$ values, indicating the accumulation of isotopically light, terrigenous OM. Sedimentation rates were probably low to moderate (less than 0.1 mm/year) because higher rates of organic matter burial (and thus higher TOC contents) are expected at higher sedimentation rates under oxic bottom water conditions (Stein, 1986).

The subsequent interval (88–77 m) might correspond roughly to the *Spinatum* zone, representing a time of sea

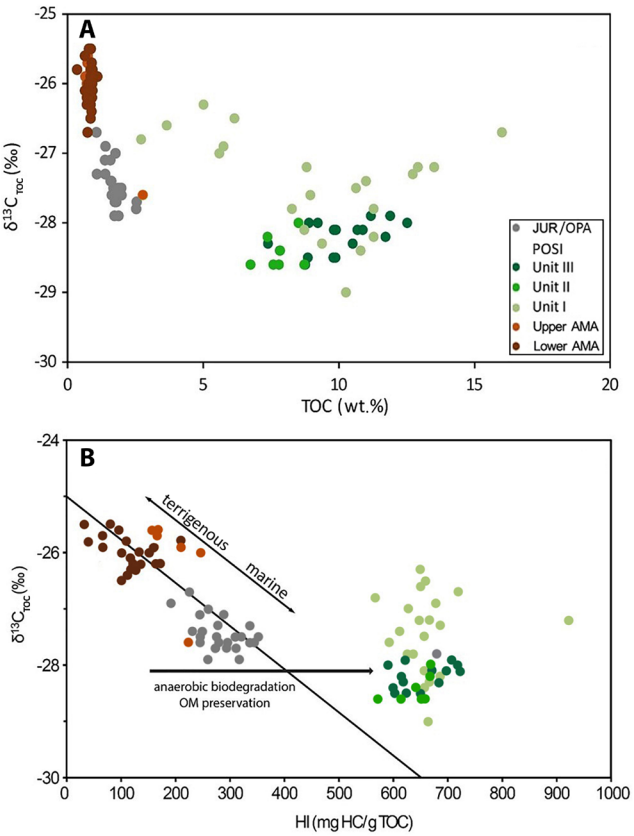

FIGURE 9 (A) Relationship between $\delta^{13}C_{TOC}$ and TOC values and (B) between $\delta^{13}C_{TOC}$ and Hydrogen Index (HI) values; see text for details. Note that some carbonate-rich samples in Unit I of the Posidonia Shale Fm are moderate in TOC (between 3 and 6 wt.%), while the remaining samples show high values (6–14 wt.%). Note that all Posidonia Shale samples show high HI values, including those with only moderate TOC content.

level fall and possibly cooler climatic conditions (van de Schootbrugge et al., 2019). It is marked by the lowest HI values in the Hunzen core. Also, TOC and TS contents are low. According to published osmium isotope data (Cohen et al., 2004), weathering intensity may have reached a minimum at the end of the Pliensbachian, probably leading to less nutrient input to the sea and lower primary productivity, which is in line with the low HI and TOC values.

The uppermost part of the organic matter-lean interval (77–72.55 m) comprises low TOC (0.9 wt%) and TIC values (1.22 wt%), except for the uppermost 10 centimetres (Figure 2; Table S1). However, HI values are slightly higher than in the underlying interval (88–77 m) and resemble those of the lowermost drilled interval (100–88 m). During the earliest Toarcian, global temperatures probably started to increase, possibly caused by the onset of large-scale Karoo-Ferrar magmatism (Pálfy & Smith, 2000) and sea level rise led to flooding of coastal areas. The interval from ~72.65–72.50 m is characterised by a gradual transition towards the Posidonia Shale Fm., marked by increasing TOC, TIC and HI values. A hiatus, or several hiati that have been reported at other locations (e.g. Hondelage Section, Marten et al. (2024); NWGB), makes it difficult to study the onset of sapropel deposition.

4.3.2 | Posidonia Shale Fm

The Posidonia Shale Fm generally plots above or close to the normal marine line (TOC/TS = 2.8; Figure 5C), indicating deposition under marine bottom waters, in which hydrogen sulfide (H_2S) formation is TOC-dependent (Littke et al., 1991). A positive intercept of the TOC/TS regression line suggests anoxic conditions with H_2S in the bottom water of the NWGB during the deposition of the Posidonia Shale Fm. In addition, the TOC-TS-Fe plot and DOP values (Figure 5D) reveal that the Posidonia Shale plots clearly in the field of anoxia, even with a small amount of excess sulphur, which may be present as organic sulphur. This data indicates pyrite formation under reducing, sulfidic bottom waters. This is in agreement with long-term euxinic conditions during the Toarcian CIE and post-CIE intervals in NW Germany, as suggested by McArthur et al. (2008). The average data of the Posidonia Shale from MAI are similar to those at Hunzen (Figure 5C); TOC values are slightly lower due to hydrocarbon generation and TS values, not affected by maturation, are slightly higher (see also Figure 5D).

Enrichment of V, U and Mo is commonly used to differentiate suboxic from anoxic/euxinic environments. In this study, high Mo_{EF} (EF >20) and TOC/P ratios, in combination with moderate U_{EF} (EF >3) (Figures 7B,C and 8) suggest anoxic to suboxic conditions during the deposition of the Posidonia Shale Fm (Jochum et al., 1995; Tribovillard et al., 2006). Furthermore, the enrichment of transition metals, like Ni and Cu, observed in the black shales is linked to their fixation in pyrite under reducing conditions. The data indicate syngenetic or early diagenetic pyrite formation, implying the presence of euxinic conditions (Figure 7A). Ag enrichment, probably associated with pyrite formation, further supports this interpretation (Figure 3).

The Mo/TOC ratio is a key proxy for evaluating salinity, redox conditions and water column stratification in depositional environments (Figure 7C). Mo is frequently used as a proxy for redox conditions and water mass restriction in marine sediments (Algeo & Maynard, 2008; Berner et al., 2013). Mo enrichment correlates with TOC content when TOC is below a certain threshold (Tribovillard et al., 2006), making the Mo/TOC ratio useful for assessing water mass restriction and Mo renewal rates via global ocean exchange (Algeo & Lyons, 2006). Threshold values for TOC in recent anoxic basins vary: 6.2 wt% in the modern Cariaco Basin, 6.1 wt% in the Black Sea, 3.2 wt% in the Saanich Inlet and up to 11.6 wt% in the Framvaren Fjord. The analysis of redox-sensitive trace metals (Mo, U, V) compared to TOC from the studied well section (Figure 7B,C) reveals overall a very restricted water body, probably similar to the present-day Black Sea. Average values for the immature Posidonia Shale at MAI are in the same range as those observed here (Figure 7B,C); TOC and Mo values are slightly higher there.

In summary, strong basin restriction during the T-OAE probably led to water column stratification and restricted circulation. Ga concentration drops sharply above the Amaltheenton Fm and remains low within the Posidonia Shale Fm (Figure 8), a typical feature of fully marine conditions (Wu et al., 2025). Fully marine conditions for the Posidonia Shale Fm are also suggested by significantly higher Ca/(Ca + Fe) ratios (Wu et al., 2025; Figure 8).

With respect to the distribution of SiO_2, Al_2O_3 and CaO, sediments from the Posidonia Shale Fm plot on or close to the so-called 'Average Shale line' (Figure 5B; Wedepohl, 1971, 1991). Basal Unit I is characterised by a dominance of calcium carbonate, which gradually diminishes towards the base of the Jurensismergel Fm. This trend is accompanied by increasing abundances of clay, suggesting enhanced transport of clastic material and nutrients from land to the sea. This data indicate for the entire sequence a dominance of detrital silicate, with little or no contribution from biogenic silica. Small quantities of biogenic silica may be present in Unit III, as previously noted by Kühn et al. (2001). The possibly warmer climate during black shale deposition was not accompanied by higher weathering intensity as evident from K_2O/Al_2O_3 ratios (Figure 8). This interpretation of a changed

hydrological regime as compared to the Amaltheenton Fm is further supported by CIA data. The ternary Al_2O_3-K_2O-(CaO^*+Na_2O) diagram shows that weathering intensity was highest in the Amaltheenton and Jurensismergel/Opalinuston Formations, where Al is strongly enriched, and less strong during Posidonia Shale Fm Units II–III deposition, consistent with a drier climate at that time (Figure 10A). While a more arid (and/or cooler) climate during Posidonia Shale deposition is suggested by the data, it could also result from changes in sediment provenance related to a global transgression (Marten et al., 2024; McArthur et al., 2008) and thus increased fluvial transport energy leading to stronger deposition of less weathered material compared to the underlying Amaltheenton Fm. Furthermore, the CaO versus TIC diagram demonstrates that some samples in the Posidonia Shale Fm deviate significantly from the 1:1 calcite line, indicating the presence of additional carbonate phases (e.g. siderite, ankerite or dolomite; mainly in Unit I) or detrital calcium in silicates (mainly in Unit III; Figure 10B).

Si/Al ratios tend to be higher than in the Amaltheenton Fm, showing a maximum between 60 and 50 m depth, indicating shallower water and transport of coarser siliciclastic material during deposition of Unit II in an overall regressive phase under warm and relatively dry conditions. While the end phase of Unit II coincides with a minor transgressive pulse, the Si/Al enrichment more probably reflects intensified fluvial discharge and terrigenous supply during regression (Remírez & Algeo, 2020; Suan et al., 2015). The ratio decreases again towards the top of the Posidonia Shale Fm and into the overlying Jurensismergel-/Opalinuston Fm, indicating more clay-rich sedimentation, possibly at greater water depth and in a more distal position. The Ti/Al ratio also increases at the base of the Posidonia Shale Fm up to 68 m depth and then slightly decreases (Figure 8). This finding also indicates a trend towards shallower water and/or greater proximity to land for Unit II. Moreover, the parallel trends of the Si/Al and Ti/Al ratios suggest a dominance of detrital silicate with low or absent contributions of biogenic silica (Burnaz et al., 2024). Concerning grain size, slightly lower Zr/Rb ratios in the Posidonia Shale Fm compared to the adjacent claystones (Figure 8 and Figure S2) indicate slightly lower coarse-grained detrital influx and grain-size fining, reflecting a shift to greater water depth and from higher to lower energy depositional conditions which favoured the accumulation of the organic matter-rich black shales consistent with a rising relative sea level (Burnaz et al., 2024; Hesselbo, 2008). This finding is in accordance with an assumed transgression during the Early Toarcian (Marten et al., 2024; McArthur et al., 2008). However, transgression and global temperature rise did obviously not lead to stronger weathering and an increased proportion of clay in the terrigenous material.

The T-OAE is probably associated with massive volcanism from the Karoo-Ferrar Large Igneous Province (Fantasia et al., 2018; Pálfy & Smith, 2000) which led to widespread Hg enrichment. The Hunzen well section displays moderate Hg enrichment (EF >5) which is highest at the base of Units I and II, and decreases towards Unit

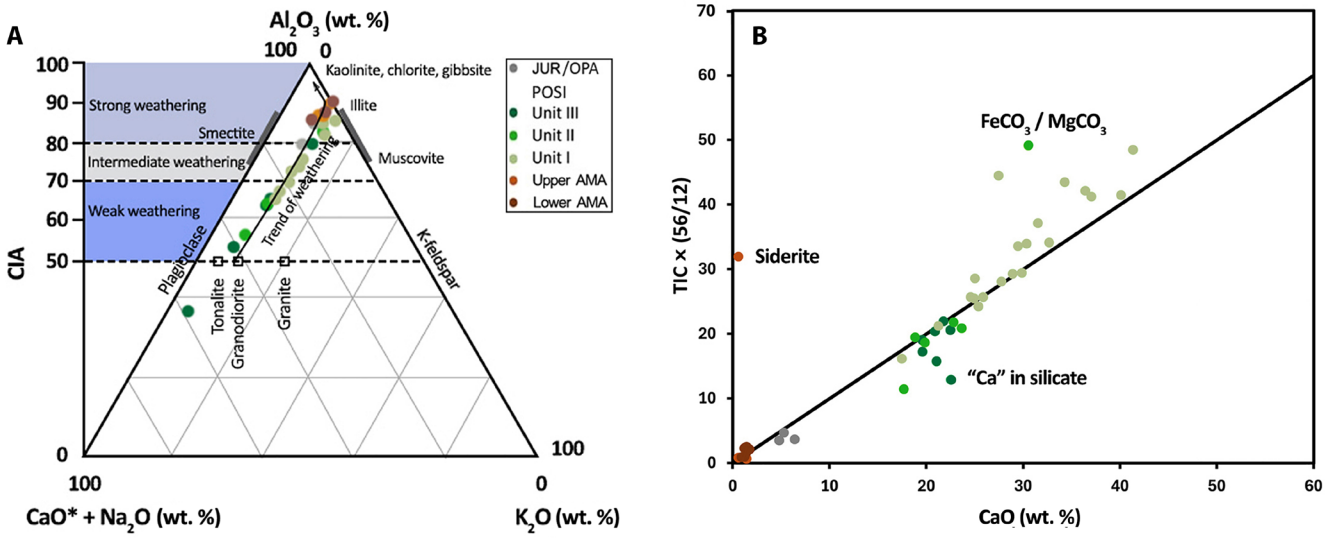

FIGURE 10 (A) Ternary diagram of Al_2O_3, K_2O and CaO (in silicates) plus Na_2O (Nesbitt & Young, 1984). Strongest weathering is indicated for samples from the Amaltheenton Fm and the Jurensismergel/Opalinuston Fm. As indicated by CIA values, weathering was least intense during deposition of Posidonia Shale Units II and III, possibly due to a drier climate; (B) CaO versus TIC×(56/12) plot. The ratio of CaO over TIC in calcite is 56/12; therefore TIC was multiplied by this factor. The 1:1 line represent pure $CaCO_3$. Samples plotting above the line indicate the presence of other carbonates, in this case probably siderite (or ankerite and dolomite, respectively). Samples plotting below the line indicate the presence of Ca in silicates or phosphates. However, phosphate content is very low.

III of the Posidonia Shale Fm (Figure 3). This trend might indicate that volcanic activity associated with LIP formation or regional volcanic sources (Fennoscandia, Sweden) decreased during the deposition of the Posidonia Shale Fm. Moreover, the stratigraphic co-occurrence of Hg enrichment with elevated TOC and TS values suggests that organic matter and sulfide sequestration may have played a significant role in Hg preservation during black shale deposition.

A dominance of marine-derived OM in the Posidonia Shale Fm, deposited under bottom water anoxia, is indicated by high HI and low OI values. In sediments with variable mixtures of hydrogen-rich marine OM and hydrogen-poor terrigenous OM, a correlation between $\delta^{13}C_{TOC}$ and HI is expected. The missing correlation for the Posidonia Shale Fm (Figure 9B) reveals the presence of mainly marine-derived OM (kerogen type II) without significant terrigenous contribution. This is also consistent with the petrographic observations. Marine aquatic macerals like tasmanites and lamalginite are prevalent in all samples (Figure 2), while terrigenous macerals (vitrinite, resedimented vitrinite and inertinite) are scarce, reinforcing the transgressional, marine palaeoenvironmental interpretation. From the upper part of Unit I towards the top of Unit III, $\delta^{13}C_{TOC}$ values remain low at about −28‰, but with a slight shift towards more positive values (by about 1‰).

The depositional environment changed significantly with the onset of the black shale formation. The Posidonia Shale Fm is characterised by high TOC contents (avg. 9.1 wt%), which are high throughout the black shale interval but lower in the carbonate-rich layers within Unit I and Unit II (e.g. at 60.65 m). Unit III has the highest TOC content (avg. 10.2 wt%) followed by Unit I (avg. 9.1 wt%). In addition, the Posidonia Shale Fm shows a higher carbonate content as compared to the over- and underlying claystones (Figures 2 and 5A). The sharp contrast in carbonate content between the Amaltheenton Fm and Posidonia Shale Fm may reflect changes in marine productivity and plankton community composition, with higher sea levels during transgression. This promotes greater dominance of calcareous marine primary producers (e.g. coccolithophores), leading to increased carbonate accumulation (Marten et al., 2024; Morard et al., 2003; Ruebsam & Al-Husseini, 2021). A warmer sea surface temperature may also have supported the proliferation of carbonate-building organisms.

A Cd/Mo ratio versus Co × Mn plot is used to infer palaeowater-column redox states (Sweere et al., 2016). The low Cd/Mo ratios and high Co × Mn values of Units I to III suggest water stratification and anoxia, leading to elevated carbon burial fluxes (Figure 11A). Unit I formed under the most extreme euxinic conditions with the longest deepwater renewal times (10^2–10^3 years), suggesting severe water column restriction. Unit II shows periodic deepwater renewal and fluctuating redox conditions. Higher Mo/TOC ratios in Unit III suggest improved circulation indicating connection to the open ocean (Figure 11B). The present findings align with those of Celestino et al. (2024) on a Posidonia Shale core drilled about 100 km further to the west, which suggests that the high organic matter content in the Lower Saxony Basin was indeed primarily driven by enhanced preservation rather than high bioproductivity.

4.3.3 | Posidonia Shale Fm—Unit I

Black shale deposition is typically linked to moderate or high bioproductivity, bottom water anoxia and moderate sedimentation rates. Unit I exhibits the highest U and Mo enrichments, indicating stable and strong bottom water anoxia. This is in agreement with high Ni_{EF}, Cu_{EF} and P_{EF} ratios, pointing to anoxic bottom water and pore water conditions under elevated OM flux, as supported by high TOC/P and U enrichment ratios (Burnaz et al., 2024; Frimmel et al., 2004; Tribovillard et al., 2006). Sundararaman et al. (1993) studied porphyrins on the nearby well Wickensen (Hils Syncline, Germany) and concluded that Unit 1 represents the most anoxic facies with the highest ratios of VO over Ni porphyrins. Also, low to moderate Mo abundances relative to U and TOC recorded in Unit I align with modern sediments deposited in the Black Sea, indicating strong basin restriction and widespread anoxia (Figure 7B,C).

The deposition of Unit I is closely associated with the onset of the T-OAE, characterised by a relative sea level rise, increased sea water temperatures, enhanced OM burial, widespread oceanic anoxia and a pronounced negative isotopic excursion (Hesselbo et al., 2000; Ruebsam et al., 2020). It should, however, be noted that the carbon isotope excursion is a rather short-term event (Figure 2, Table S1; Burnaz et al., 2024; Marten et al., 2024), while black shale deposition lasted much longer, especially in northern Germany (Ruebsam & Schwark, 2024). The higher ocean temperatures, by up to 10°C (Ruebsam et al., 2020) led to lower oxygen solubility and thus less efficient oxic degradation of organic matter (Fantasia et al., 2018; Geng & Duan, 2010; Krencker et al., 2015). Strong continental weathering is supported by multiple elemental ratios (such as Ti/Al and Zr/Rb; Figure S2), suggesting increased detrital influx from landmasses into marine basins during this time (Thibault et al., 2018; Xu et al., 2018).

In the lowermost section, Unit I is marked by a nCIE, though less prominent than in other parts of western

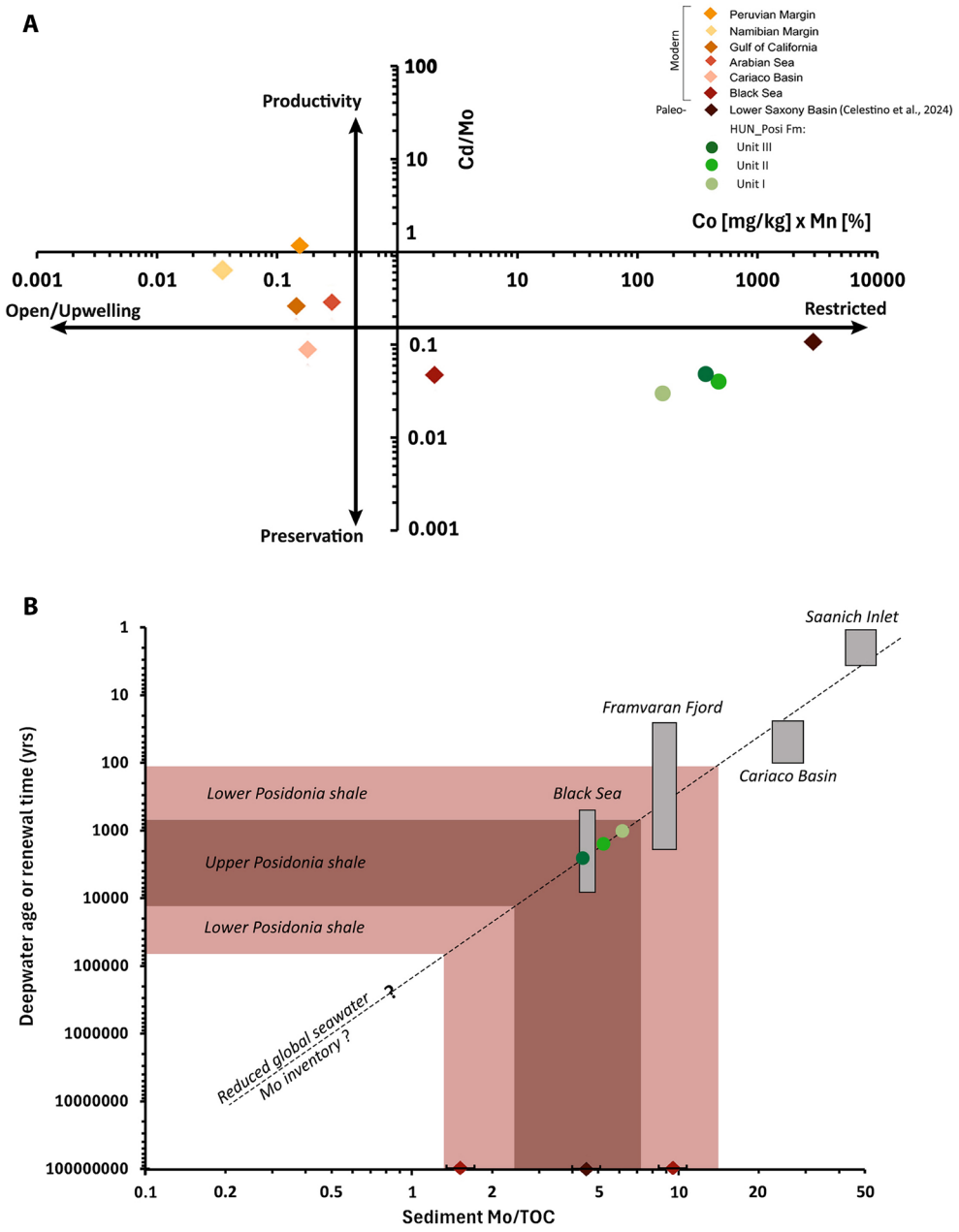

FIGURE 11 (A) Cd/Mo ratio versus Co*Mn concentrations and (B) Mo/TOC ratios of the Posidonia Shale Fm in the Hunzen Well, compared to sedimentary values in present-day and other Toarcian anoxic-euxinic depositional environments and to modern deepwater renewal times (modified after Celestino et al., 2024; Sweere et al., 2016).

Europe, such as Southern Germany and NWGB (Celestino et al., 2024; Küspert, 1982; Marten et al., 2024; Ruebsam et al., 2024; van de Schootbrugge et al., 2019). This discrepancy may reflect either a stratigraphic gap or insufficient sampling resolution that prevented capture of the complete excursion, with only the rising limb preserved in the Hunzen section. The nCIE at the base of Unit I is possibly linked to the release of isotopically light greenhouse gases from climate-sensitive reservoirs such as the cryosphere (Röhl et al., 2001; Ruebsam et al., 2019) and/or by KFLIP volcanism (Galasso et al., 2021; Hesselbo et al., 2000; Sælen et al., 2000; Them, Gill, Caruthers, et al., 2017), regional marine basin controls (Küspert, 1982), enhanced chemical weathering (Them, Gill, Caruthers, et al., 2017) or major marine turnover (van de Schootbrugge et al., 2013). Isotopic and XRF data (e.g. elevated Hg concentrations; Figure 3) suggest that both global and regional factors influenced black shale deposition.

4.3.4 | Posidonia Shale Fm—Unit II

Unit II shows indications of non-permanent bottom water anoxia, associated with the Low Carbon Zone (LCZ)

identified by Littke et al. (1991). This different pattern is possibly related to a relative sea level fall and storm waves reaching temporarily the bottom water thus hindering a persistent water stratification (Littke et al., 1991). The latter authors observed that this interval is characterised by the occurrence of bivalve-rich layers indicating at least periodically oxygenated bottom water. The presence of more oxic conditions in this interval is also in line with lower TOC, HI and Mo_{EF} values. Slightly deteriorated organic matter preservation in this unit is indicated by lower TOC (avg. 7.1 wt%) and HI values (avg. 582 mg HC/g TOC) (Figure 2). The lower HI values probably resulted from carbon loss due to bacterial alteration at or just below the sediment/water interface as proven for example, for recent sediments within the oxygen-minimum zone offshore Pakistan (Lückge et al., 1999).

A thin carbonate-rich layer (stratigraphic depth of 60.65 m) within Unit II exhibits unusually high Mo relative to TOC and U. In addition, only this layer is characterised by an exceptional, very high Si/Al ratio. As high detrital quartz in this carbonate layer is difficult to envisage, the ratio is probably related to the presence of biogenic silica derived from opal-bearing organisms. The Mo data indicate a brief period of enhanced Mo replenishment.

Interestingly, lenticular laminations and small layers of bioturbation observed in Unit II resemble features reported in carbonate-rich layers of the Posidonia Shale Fm in southern Germany, which may reflect short-term oxygenation events at the sediment–water interface (Röhl et al., 2001). Nevertheless, the overall water circulation within the basin remained restricted during deposition of Unit II (Figure 11B). According to the studies of Dotternhausen and Schesslitz sections by Röhl and Schmid-Röhl (2005), Unit II might align with the transition between the *falciferum*/*serpentinum* and *bifrons* zones in southern Germany, where abundant calcareous shells and fish debris were observed.

4.3.5 | Posidonia Shale Fm—Unit III

Unit III reflects re-established anoxic conditions towards the late Toarcian (Figure 7B). In comparison to the underlying unit, Unit III shows elevated TOC (avg. 10.2 wt%) and HI values (avg. 642 mg HC/g TOC) and a trend towards lower carbonate and higher silicate contents (Figure 2). This is evident from a plot of carbonate versus TOC (Figure 5A), which shows a negative correlation for Units I and III. This unit represents overall deeper water with more clastic input from the continents, including silicate and nutrients. K_2O/Al_2O_3 ratios begin to decrease (Figure 8), probably due to a shift back towards more humid conditions and enhanced weathering. Probably, both primary productivity and OM preservation were stimulated during times of enhanced supply of nutrients from land. This is also expressed by the highest TOC and HI values observed in the entire profile (Figures 2 and 6; Figure S1; Table 1). During deposition of Unit III, water column stratification persisted (Figure 11, Figure S2), even without any global anoxia (Frimmel et al., 2004). Based on Mo and U data (Figure 7B,C), Unit III shows moderate to strong basin restriction in line with trends observed in coeval strata of the NW German Basin (Celestino et al., 2024). The redox conditions inferred from these trace metal enrichments are also similar to those found in modern restricted basins such as the Framvaren Fjord and the Black Sea (e.g. Algeo & Lyons, 2006). This is in line with TS/TOC/Fe data (Figure 5D), suggesting a shift back towards more euxinic conditions.

The uppermost part of Unit III is marked by erosional features, probably due to reworking processes linked to the subsequent transgressive cycle of the Upper Toarcian Jurensismergel Fm (Figure S1). In the NWGB, Unit III is comparatively thick (about 18 m in the Hunzen well) as compared to the SWGB, where erosional gaps often lead to its absence (Celestino et al., 2024). The greater thickness of the black shale in the NWGB suggests higher subsidence and sedimentation rates and/or longer duration of sedimentation, contrasting with the stratigraphic gaps in areas of lower subsidence or shallower water depth in southern Germany.

4.3.6 | Jurensismergel-/Opalinuston Fm

The transition from the Posidonia Shale Fm to the Jurensismergel Fm is marked by declining TOC, TIC, HI values and elevated OI values, indicating that bottom waters became less reducing and conditions less favourable for OM preservation (Figure 2) (Littke et al., 1991). The higher TOC content (avg. 1.8 wt%) and HI values (avg. 300 mg HC/g TOC) of the Jurensismergel Fm compared to the Amaltheenton Fm suggest that the depositional environment remained at least suboxic (Figures 5D, 8 and 12). The Jurensismergel Fm shows moderate TS content, but rather low TOC/TS ratios (Figure 5C). This suggests that depositional conditions remained oxygen-deficient after the Lower Toarcian black shale deposition (McArthur et al., 2008). Suboxic conditions are also indicated by Fe/TS ratios (Figure 5D). Ga contents are surprisingly high, indicating that conditions were no longer fully marine (Figure 8), which is also indicated by low Sr contents and Sr/Ba ratios (Figure S2C).

Lower $\delta^{13}C_{TOC}$ as well as higher HI and TOC values (Figure 9A,B) of the Jurensismergel Fm compared to the underlying Amaltheenton Fm suggest a greater contribution of marine over terrigenous organic matter, which is in line with the observation of abundant liptinite

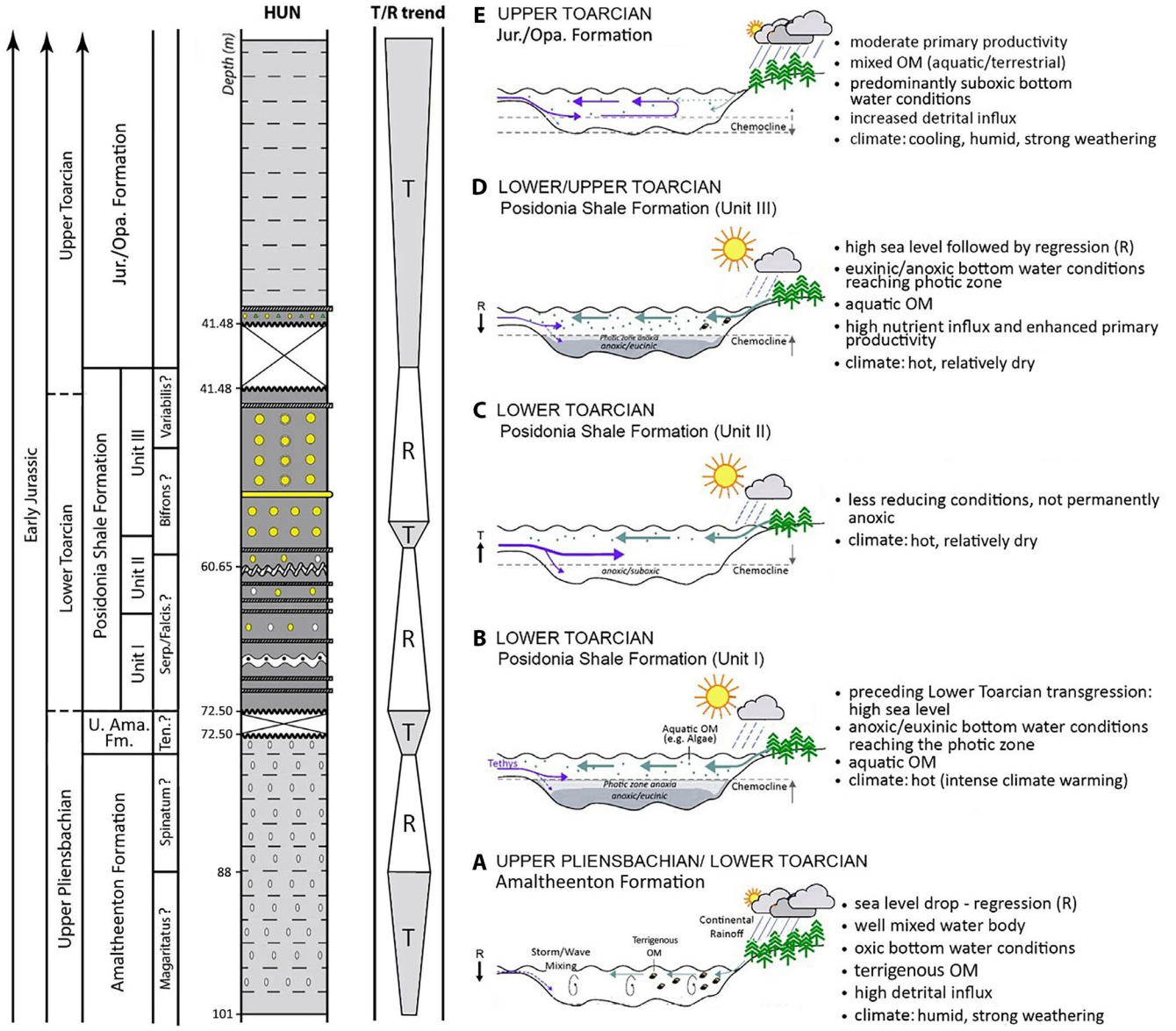

FIGURE 12 Lithostratigraphic profile of HUN with schematic regression-transgression (T/R) cyclicity (left) and chronological depositional model (right) (modified after Burnaz et al., 2024).

(Figure 2). The data thus indicate that the Jurensismergel Fm contains mixed terrigenous and marine organic matter, in contrast to the Posidonia Shale Fm in which the organic matter is almost exclusively marine derived. The relationship between HI and $\delta^{13}C_{TOC}$ values (Figure 9B) clearly indicates mixed OM sources with a higher marine contribution compared to the Amaltheenton Fm, reflecting enhanced marine productivity and/or improved basin connectivity, which could have facilitated the exchange of nutrients and planktonic communities with the open ocean.

The Si/Al, Ti/Al and Zr/Rb ratios of the Jurensismergel Fm are relatively low at the base, followed by an increase towards values similar to those of the Posidonia Shale Fm and Amaltheenton Fm. Overall, there is only a little variability of these ratios, indicating constant inflow of clastic material into the sea. In contrast, the Jurensismergel Fm shows higher calcium carbonate contents compared to the Amatheenton Fm. This formation plots near the clay mineral apex (Figure 5B), indicative of fine-grained sediments deposited during times of high terrigenous input into marine environments.

Following the erosive top marked by the conglomerate above the Posidonia Shale Fm (Figure 4C), the Jurensismergel Fm is best explained by a transgressive event marked by a flooding surface. Rather cool and humid climatic conditions may have led to lower surface-water temperatures (~6–7°C cooler than before) and strong freshwater influx, facilitating bottom-water reoxygenation (Dera et al., 2009).

5 | CONCLUSION

The Hunzen well section was recently drilled at the southern limb of the Hils Syncline in the Lower Saxony Basin and provides novel and valuable insights into the palaeodepositional and palaeoenvironmental evolution of the Upper Pliensbachian to Upper Toarcian/Aalenian. The well reached a depth of about 100 m recovering three clearly distinct lithological formations: the Amaltheenton Fm, the Posidonia Shale Fm and the Jurensismergel-/Opalinuston Fm. These formations reached the early stage of oil generation with maximum burial temperatures of about 90–100°C. Lithostratigraphic, geochemical and organic petrological data reveal significant environmental changes during the deposition of the three formations. Transgressive-regressive cycles were identified, highlighting both short- and long-term variations in sea level and redox conditions, providing a basis for establishing the palaeodepositional model.

- The Amaltheenton Fm was deposited in a shallow marine setting under persistent oxygenated bottom-water conditions. Strong terrigenous material input under a humid climate and strong weathering led to the deposition of clay-rich, TOC-lean sediments depleted in elements such as K, Na and Ca. A regression resulted in a shift towards shallow marine conditions and the deposition of coarser-grained, but still clay-dominated intercalations, with TOC showing the lowest values of the investigated sequence. In the uppermost part of the Amaltheenton Fm, a transgressive trend is observed in the data set.
- Strong Lower Toarcian transgression possibly related to global warming led to the deposition of the Posidonia Shale Fm characterised by exceptionally high TOC contents (~9 wt%) and carbonate contents (~50 wt%). Only the lowermost 50 cm of the 30 m thick unit are characterised by a negative carbon isotope excursion. A very warm climate is assumed for this interval, but based on geochemical proxies—weathering intensity was less pronounced than during deposition of the shales below and above, pointing to a drier climate during the Lower Toarcian in Central Europe. The three distinct sub-units of the Posidonia Shale Fm reflect different stages of anoxia, marine productivity and sediment influx, but organic matter is hydrogen-rich and of marine origin in all units. Unit I is characterised by a short-lived transgression and strong, persistent bottom water anoxia. This unit represents the well-known Toarcian Oceanic Anoxic Event (Jenkyns Event, about 183 Ma). Unit II represents a short-time regression with periodic, short-term bottom-water oxygenation and more rigorous mixing of the water column due to storm waves. TOC contents and HI values, while still being high, are lower compared to Units I and III. In Unit III, a transgressive phase increased continental runoff and nutrient supply, boosting marine productivity. Persistent bottom water anoxia was also re-established. Additionally, the connection with the Tethys and the Arctic Sea may have played a role in influencing water chemistry, water stratification and circulation patterns.
- The Jurensismergel Fm was deposited under humid conditions with increased continental weathering and favourable OM preservation. Improved basin-ocean connectivity facilitated periodic bottom-water oxygenation, marking the end of widespread black shale deposition in the Northwest German Basin and elsewhere in Central Europe. The TOC content (~2 wt%) and HI values (~283 mg HC/g TOC) are moderate while organic matter composition shifted to a mix of marine and terrigenous sources.
- The black shale deposition of the Posidonia Shale Fm was controlled by a combination of regional (OM productivity, water mass restriction, nutrient influx, monsoonal activity) and global (greenhouse climate, oxygen depletion in warm waters) factors. The origin of the Hg anomaly, which may potentially be linked to the Karoo-Ferrar volcanism, remains uncertain. This study highlights the complex interplay of global and regional controls in shaping Early Jurassic palaeoenvironments and the deposition of the Posidonia Shale Fm in the Northwest German Basin.

ACKNOWLEDGEMENTS

We thank the German Federal Company for the Disposal of Radioactive Waste (BGE) and the German Federal Ministry for Economic Affairs and Climate Action (BMWK) for funding the MATURITY project through grant 02E11931 awarded to R.L., J.E. and F.A, which made the drilling of fresh core material possible. We thank two reviewers for constructive comments on an earlier draft of this manuscript and the following people for their highly appreciated contribution to the measurements and sample preparation: G. Scheeder, Y. Meve and L. Elzer (all BGR; $\delta^{13}C_{TOC}$); R. Koch and R. Lippmann (both LBEG; core description); D. Macherey (RWTH Aachen University; preparation of polished sections for microscopy). Open Access funding enabled and organized by Projekt DEAL.

CONFLICT OF INTEREST STATEMENT

We declare that we have no financial and personal relationships with other people or organisations that can inappropriately influence our work, and there is no professional or other personal interest of any nature or kind in any product, service and/or company that could be construed as influencing the content of this paper.

DATA AVAILABILITY STATEMENT

The authors confirm that the data supporting the findings of this study are available within the article and its Supporting Information: Figures S1 and S2; Tables S1 and S2.

ORCID

Premila Wijesinghe https://orcid.org/0000-0003-1972-5047
Ralf Littke https://orcid.org/0000-0003-0421-8720
Martin Blumenberg https://orcid.org/0000-0002-9791-8568
Thomas Mann https://orcid.org/0000-0002-9182-2741
Thorsten Bauersachs https://orcid.org/0000-0003-4858-9443

REFERENCES

Ajuaba, S., Sachsenhofer, R.F., Bechtel, A., Galasso, F., Gross, D., Misch, D. & Schneebeli-Hermann, E. (2022) Biomarker and compound-specific isotope records across the Toarcian CIE at the Dormettingen section in SW Germany. *International Journal of Earth Sciences*, 111, 1631–1661.

Ajuaba, S., Sachsenhofer, R.F., Galasso, F., Garlichs, T.U., Gross, D., Schneebeli-Hermann, E., Misch, D. & Oriabure, J.E. (2024) The Toarcian Posidonia Shale at Salem (North Alpine Foreland Basin; South Germany): hydrocarbon potential and paleogeography. *International Journal of Earth Sciences*, 113, 1–38.

Algeo, T.J. & Lyons, T.W. (2006) Mo-total organic carbon covariation in modern anoxic marine environments: implications for analysis of paleoredox and paleohydrographic conditions. *Paleoceanography*, 21, 2004PA001112.

Algeo, T.J. & Maynard, J.B. (2008) Trace-metal covariation as a guide to water-mass conditions in ancient anoxic marine environments. *Geosphere*, 4, 872–887.

Algeo, T.J. & Tribovillard, N. (2009) Environmental analysis of paleoceanographic systems based on molybdenum–uranium covariation. *Chemical Geology*, 268, 211–225.

Arp, G., Balmuk, Y., Seppelt, S. & Reimer, A. (2023) Biostratigraphy and sedimentary sequences of the Toarcian Hainberg section (Northwestern Harz foreland, Northern Germany). *Zitteliana*, 97, 1–27.

Arp, G. & Gropengießer, S. (2016) The Monotis–Dactylioceras Bed in the Posidonienschiefer Formation (Toarcian, southern Germany): condensed section, tempestite, or tsunami-generated deposit? *PalZ*, 90, 271–286.

Arp, G., Gropengießer, S., Schulbert, C., Jung, D. & Reimer, A. (2021) Biostratigraphy and sequence stratigraphy of the toarcian ludwigskanal section (franconian alb, southern Germany). *Zitteliana*, 95, 57–94.

Behar, F., Beaumont, V. & Penteado, H.D.B. (2001) Rock-Eval 6 technology: performances and developments. *Oil & Gas Science and Technology*, 56, 111–134.

Bern, C.R., Walton-Day, K. & Naftz, D.L. (2019) Improved enrichment factor calculations through principal component analysis: examples from soils near breccia pipe uranium mines, Arizona, USA. *Environmental Pollution*, 248, 90–100.

Berner, R.A. (1984) Sedimentary pyrite formation—an update. *Geochimica et Cosmochimica Acta*, 48, 605–615.

Berner, R.A. & Raiswell, R. (1984) C/S method for distinguishing freshwater from marine sedimentary rocks. *Geology*, 12, 365–368.

Berner, Z.A., Puchelt, H., Nöltner, T. & Kramar, U. (2013) Pyrite geochemistry in the Toarcian Posidonia Shale of south-west Germany: evidence for contrasting trace-element patterns of diagenetic and syngenetic pyrites. *Sedimentology*, 60, 548–573.

Betz, D., Fuhrer, F., Greiner, G. & Plein, E. (1987) Evolution of the Lower Saxony Basin. *Tectonophysics*, 137, 127–170.

Burnaz, L., Littke, R., Grohmann, S., Erbacher, J., Strauss, H. & Amann, F. (2024) Lower Jurassic (Pliensbachian-Toarcian) marine paleoenvironment in Western Europe: sedimentology, geochemistry and organic petrology of the wells Mainzholzen and Wickensen, Hils Syncline, Lower Saxony Basin. *International Journal of Earth Sciences*, 113, 1999–2022.

Canfield, D.E., Raiswell, R. & Bottrell, S. (1992) The reactivity of sedimentary iron minerals toward sulfide. *American Journal of Science*, 292, 659–683.

Celestino, R.F.S., Ruhl, M., Dickson, A.J., Idiz, E., Jenkyns, H.C., Leng, M.J., Mattioli, E., Minisini, D. & Hesselbo, S.P. (2024) Protracted carbon burial following the Early Jurassic Toarcian Oceanic Anoxic Event (Posidonia Shale, Lower Saxony Basin, Germany). *International Journal of Earth Sciences*, 113, 2023–2041.

Cohen, A.S., Coe, A.L., Harding, S.M. & Schwark, L. (2004) Osmium isotope evidence for the regulation of atmospheric CO_2 by continental weathering. *Geology*, 32, 157–160.

Curtis, C., Coleman, M. & Love, L. (1986) Pore water evolution during sediment burial from isotopic and mineral chemistry of calcite, dolomite and siderite concretions. *Geochimica et Cosmochimica Acta*, 50, 2321–2334.

Dean, W.E. & Arthur, M.A. (1989) Iron-sulfur-carbon relationships in organic-carbon-rich sequences; I, Cretaceous Western Interior Seaway. *American Journal of Science*, 289, 708–743.

Dean, W.E. & Gardner, J.V. (1998) Pleistocene to Holocene contrasts in organic matter production and preservation on the California continental margin. *Geological Society of America Bulletin*, 110, 888–899.

Dera, G., Pucéat, E., Pellenard, P., Neige, P., Delsate, D., Joachimski, M.M., Reisberg, L. & Martinez, M. (2009) Water mass exchange and variations in seawater temperature in the NW Tethys during the Early Jurassic: evidence from neodymium and oxygen isotopes of fish teeth and belemnites. *Earth and Planetary Science Letters*, 286, 198–207.

Fang, R.H., Littke, R., Zieger, L., Baniasad, A., Li, M.J. & Schwarzbauer, J. (2019) Changes of composition and content of tricyclic terpane, hopane, sterane, and aromatic biomarkers throughout the oil window: a detailed study on maturity parameters of Lower Toarcian Posidonia Shale of the Hils Syncline, NW Germany. *Organic Geochemistry*, 138, 103928.

Fantasia, A., Föllmi, K.B., Adatte, T., Bernárdez, E., Spangenberg, J.E. & Mattioli, E. (2018) The Toarcian oceanic anoxic event in southwestern Gondwana: an example from the Andean Basin, northern Chile. *Journal of the Geological Society*, 175, 883–902.

Fantasia, A., Follmi, K.B., Adatte, T., Spangenberg, J.E. & Mattioli, E. (2019) Expression of the Toarcian Oceanic Anoxic Event: new insights from a Swiss transect. *Sedimentology*, 66, 262–284.

Fischer, R., Jäger, M., Konstantinopoulou, A., Kristan-Tollmann, E., Luppold, W. & Ohm, H.-H. (1986) Paläontologie einer

epikontinentalen Lias-Schichtfolge: oberes Sinemirium bis Oberes Domerium von Empelde bei Hannover. *Facies*, 15, 53–175.

Frimmel, A., Oschmann, W. & Schwark, L. (2004) Chemostratigraphy of the posidonia Black Shale, SW Germany I. Influence of sea-level variation on organic facies evolution. *Chemical Geology*, 206, 199–230.

Galasso, F., Schmid-Röhl, A., Feist-Burkhardt, S., Bernasconi, S.M. & Schneebeli-Hermann, E. (2021) Changes in organic matter composition during the Toarcian Oceanic Anoxic Event (T-OAE) in the Posidonia Shale Formation from Dormettingen (SW-Germany). *Palaeogeography Palaeoclimatology Palaeoecology*, 569, 110327.

Gaupp, R., Voigt, T., Lützner, H., Müller, H. & Føhlisch, K. (1998) Stratigraphy and sedimentological evolution of Lower and Middle Triassic deposits in the SE part of the Germanic Triassic Basin. Excursions of the International Symposium on the Epicontinental Triassic, Halle (Saale), 99–120.

Gaus, G., Hoyer, E.M., Seemann, T., Fink, R., Amann, F. & Littke, R. (2022) Laboratory investigation of permeability, pore space and unconfined compressive strength of uplifted Jurassic mudstones: the role of burial depth and thermal maturation. *Zeitschrift der Deutschen Gesellschaft für Geowissenschaften*, 173, 469–489.

Geng, M. & Duan, Z.H. (2010) Prediction of oxygen solubility in pure water and brines up to high temperatures and pressures. *Geochimica et Cosmochimica Acta*, 74, 5631–5640.

Grohmann, S., Littke, R., Abu-Mahfouz, I., Gaus, G., Klaver, J., Thüns, N., Schulte, P., Patzek, T. & Vahrenkamp, V. (2023) The deposition of type II-S Jordan oil shale in the context of Late Cretaceous source rock formation in the Eastern Mediterranean realm. Insights from organic and inorganic geochemistry and petrography. *Marine and Petroleum Geology*, 148, 106058.

Harries, P.J. & Little, C.T. (1999) The early Toarcian (Early Jurassic) and the Cenomanian–Turonian (Late Cretaceous) mass extinctions: similarities and contrasts. *Palaeogeography, Palaeoclimatology, Palaeoecology*, 154, 39–66.

Hart, B.S. & Hofmann, M.H. (2022) Revisiting paleoenvironmental analyses and interpretations of organic-rich deposits: the importance of TOC corrections. *Organic Geochemistry*, 170, 104434.

Hesselbo, S.P. (2008) Sequence stratigraphy and inferred relative sea-level change from the onshore British Jurassic. *Proceedings of the Geologists' Association*, 119, 19–34.

Hesselbo, S.P., Gröcke, D.R., Jenkyns, H.C., Bjerrum, C.J., Farrimond, P., Bell, H.S.M. & Green, O.R. (2000) Massive dissociation of gas hydrate during a Jurassic oceanic anoxic event. *Nature*, 406, 392–395.

Hesselbo, S.P., Jenkyns, H.C., Duarte, L.V. & Oliveira, L.C.V. (2007) Carbon-isotope record of the Early Jurassic (Toarcian) Oceanic Anoxic Event from fossil wood and marine carbonate (Lusitanian Basin, Portugal). *Earth and Planetary Science Letters*, 253, 455–470.

Jarvis, I., Atar, E., Gröcke, D.R., Herringshaw, L.G. & Trabucho-Alexandre, J.P. (2024) A global reference for black shale geochemistry and the T-OAE revisited: upper Pliensbachian–middle Toarcian (Lower Jurassic) chemostratigraphy in the Cleveland Basin, England. *Geological Magazine*, 161, e13.

Jenkyns, H.C. (1988) The early Toarcian (Jurassic) anoxic event; stratigraphic, sedimentary and geochemical evidence. *American Journal of Science*, 288, 101–151.

Jenkyns, H.C. (2010) Geochemistry of oceanic anoxic events. *Geochemistry, Geophysics, Geosystems*, 11, 2009GC002788.

Jochum, J., Friedrich, G., Leythaeuser, D. & Littke, R. (1995) Intraformational Redistribution of Selected Trace-Elements in the Posidonia Shale (Hils Syncline, Nw Germany) Caused by the Thermal Influence of the Vlotho Massif. *Ore Geology Reviews*, 9, 353–362.

Kemp, D.B., Coe, A.L., Cohen, A.S. & Schwark, L. (2005) Astronomical pacing of methane release in the Early Jurassic period. *Nature*, 437, 396–399.

Kemp, D.B., Suan, G., Fantasia, A., Jin, S. & Chen, W. (2022) Global organic carbon burial during the Toarcian oceanic anoxic event: patterns and controls. *Earth-Science Reviews*, 231, 104086.

Krencker, F.N., Bodin, S., Suan, G., Heimhofer, U., Kabiri, L. & Immenhauser, A. (2015) Toarcian extreme warmth led to tropical cyclone intensification. *Earth and Planetary Science Letters*, 425, 120–130.

Kühn, V., Heydemann, A. & Usdowski, E. (2001) Mineralogy of the Upper Albian sediments from the Kirchrode I borehole with special emphasis on the clay mineralogy. *Palaeogeography Palaeoclimatology Palaeoecology*, 174, 145–159.

Küspert, W. (1982) *Environmental changes during oil shale deposition as deduced from stable isotope ratios. Cyclic and event stratification*. Heidelberg: Springer.

Lehmann, M.F., Bernasconi, S.M., Barbieri, A. & Mckenzie, J.A. (2002) Preservation of organic matter and alteration of its carbon and nitrogen isotope composition during simulated and in situ early sedimentary diagenesis. *Geochimica et Cosmochimica Acta*, 66, 3573–3584.

Lis, K., Wojtulek, P., Lis, G. & Jelonek, I. (2022) Terrigenous organic matter and formation of siderite in the Bathonian Ore-Bearing Clay Formation at Gnaszyn, Poland—a petrochemical study. *Annales Societatis Geologorum Poloniae*, 92, 295–312. https://doi.org/10.14241/asgp.2022.09

Littke, R., Baker, D.R., Leythaeuser, D. & Rullkötter, J. (1991) Keys to the depositional history of the Posidonia Shale (Toarcian) in the Hils Syncline, Northern Germany. *Modern and Ancient Continental Shelf Anoxia*, 58, 311–333.

Littke, R., Bayer, U., Gajewski, D. & Nelskamp, S. (2008) *Dynamics of complex intracontinental basins: the central European basin system*. Berlin: Springer.

Loh, H., Maul, B., Prauss, M. & Riegel, W. (1986) Primary production, maceral formation and carbonate species in the Posidonia Shale of NW Germany. *Mitteilungen Aus Dem Geologisch-Paläontologischen Institut Der Universität Hamburg*, 60, 397–421.

Lokhorst, A., Gerling, P., Laier, T., Nicholson, R. & Pokorski, J. (1996) Atlas of the composition and isotope ratios of natural gasses in Northwest European gas fields. 58th EAGE Conference and Exhibition, European Association of Geoscientists & Engineers, cp-48-00374.

Lückge, A., Ercegovac, M., Strauss, H. & Littke, R. (1999) Early diagenetic alteration of organic matter by sulfate reduction in Quaternary sediments from the northeastern Arabian Sea. *Marine Geology*, 158, 1–13.

Marten, T., Ruebsam, W., Mutterlose, J., Wiesenberg, G.L.B. & Schwark, L. (2024) Latest Pliensbachian to Early Toarcian depositional environment and organo-facies evolution in the North-German Basin (Hondelage Section). *International Journal of Earth Sciences*, 113, 2043–2064.

McArthur, J.M., Algeo, T.J., van de Schootbrugge, B., Li, Q. & Howarth, R.J. (2008) Basinal restriction, black shales, Re-Os dating, and the Early Toarcian (Jurassic) oceanic anoxic event. *Paleoceanography*, 23, 2008PA001607.

McElwain, J.C., Wade-Murphy, J. & Hesselbo, S.P. (2005) Changes in carbon dioxide during an oceanic anoxic event linked to intrusion into Gondwana coals. *Nature*, 435, 479–482.

Merkel, A. & Munnecke, A. (2023) Glendonite-bearing concretions from the upper Pliensbachian (Lower Jurassic) of South Germany: indicators for a massive cooling in the European epicontinental sea. *Facies*, 69, 10.

Meschede, M. & Warr, L.N. (2019) *The geology of Germany: a process-oriented approach*. Berlin: Springer.

Morard, A., Guex, J., Bartolini, A., Morettini, E. & de Wever, P. (2003) A new scenario for the Domerian-Toarcian transition. *Bulletin De La Société Géologique De France*, 174, 351–356.

Mutterlose, J., Klopschar, M. & Visentin, S. (2022) Ecological adaptation of marine floras and faunas across the Early Jurassic Toarcian Oceanic Anoxic Event–A case study from northern Germany. *Palaeogeography, Palaeoclimatology, Palaeoecology*, 602, 111176.

Nesbitt, H.W. & Young, G.M. (1984) Prediction of some weathering trends of plutonic and volcanic rocks based on thermodynamic and kinetic considerations. *Geochimica et Cosmochimica Acta*, 48, 1523–1534.

Pálfy, J.Z. & Smith, P.L. (2000) Synchrony between Early Jurassic extinction, oceanic anoxic event, and the Karoo-Ferrar flood basalt volcanism. *Geology*, 28, 747–750.

Parrish, J.T. (1993) Climate of the supercontinent Pangea. *Journal of Geology*, 101, 215–233.

Pillot, D., Deville, E. & Prinzhofer, A. (2014) Identification and quantification of carbonate species using Rock-Eval pyrolysis. *Oil & Gas Science and Technology–Revue d'IFP Energies Nouvelles*, 69, 341–349.

Plet, C., Grice, K., Pagès, A., Ruebsam, W., Coolen, M. & Schwark, L. (2016) Microbially-mediated fossil-bearing carbonate concretions and their significance for palaeoenvironmental reconstructions: a multi-proxy organic and inorganic geochemical appraisal. *Chemical Geology*, 426, 95–108.

Rachold, V. & Brumsack, H.J. (2001) Inorganic geochemistry of Albian sediments from the Lower Saxony Basin NW Germany: palaeoenvironmental constraints and orbital cycles. *Palaeogeography, Palaeoclimatology, Palaeoecology*, 174, 121–143.

Raiswell, R. & Fisher, Q.J. (2000) Mudrock-hosted carbonate concretions: a review of growth mechanisms and their influence on chemical and isotopic composition. *Journal of the Geological Society*, 157, 239–251.

Remírez, M.N. & Algeo, T.J. (2020) Paleosalinity determination in ancient epicontinental seas: a case study of the T-OAE in the Cleveland Basin (UK). *Earth-Science Reviews*, 201, 103072.

Röhl, H.-J. & Schmid-Röhl, A. (2005) Lower Toarcian (Upper Liassic) black shales of the Central European epicontinental basin: a sequence stratigraphic case study from the SW German Posidonia Shale.

Röhl, H.J., Schmid-Röhl, A., Oschmann, W., Frimmel, A. & Schwark, L. (2001) The Posidonia Shale (Lower Toarcian) of SW-Germany:: an oxygen-depleted ecosystem controlled by sea level and palaeoclimate. *Palaeogeography Palaeoclimatology Palaeoecology*, 165, 27–52.

Rowe, H.D., Loucks, R.G., Ruppel, S.C. & Rimmer, S.M. (2008) Mississippian Barnett Formation, Fort Worth Basin, Texas: Bulk geochemical inferences and Mo–TOC constraints on the severity of hydrographic restriction. *Chemical Geology*, 257, 16–25.

Ruebsam, W. & Al-Husseini, M. (2021) Orbitally synchronized late Pliensbachian-early Toarcian glacio-eustatic and carbon-isotope cycles. *Palaeogeography Palaeoclimatology Palaeoecology*, 577, 110562.

Ruebsam, W., Franz, M., Ansorge, J., Obst, K. & Schwark, L. (2024) Late Triassic to Early Jurassic carbon isotope chemostratigraphy and organo-facies evolution in a distal to proximal transect of the North German Basin. *International Journal of Earth Sciences*, 113, 1977–1998.

Ruebsam, W., Mattioli, E. & Schwark, L. (2022) Weakening of the biological pump induced by a biocalcification crisis during the early Toarcian Oceanic Anoxic Event. *Global and Planetary Change*, 217, 103954.

Ruebsam, W., Mayer, B. & Schwark, L. (2019) Cryosphere carbon dynamics control early Toarcian global warming and sea level evolution. *Global and Planetary Change*, 172, 440–453.

Ruebsam, W., Reolid, M., Sabatino, N., Masetti, D. & Schwark, L. (2020) Molecular paleothermometry of the early Toarcian climate perturbation. *Global and Planetary Change*, 195, 103351.

Ruebsam, W. & Schwark, L. (2024) Disparity between Toarcian Oceanic Anoxic Event and Toarcian carbon isotope excursion. *International Journal of Earth Sciences*, 113, 2065–2076.

Rullkötter, J., Leythaeuser, D., Horsfield, B., Littke, R., Mann, U., Muller, P.J., Radke, M., Schaefer, R.G., Schenk, H.J., Schwochau, K., Witte, E.G. & Welte, D.H. (1988) Organic-matter maturation under the influence of a deep intrusive heat-source—a natural experiment for quantitation of hydrocarbon generation and expulsion from a petroleum source rock (Toarcian Shale, Northern Germany). *Organic Geochemistry*, 13, 847–856.

Sælen, G., Tyson, R.V., Telnæs, N. & Talbot, M.R. (2000) Contrasting watermass conditions during deposition of the Whitby Mudstone (Lower Jurassic) and Kimmeridge Clay (Upper Jurassic) formations, UK. *Palaeogeography Palaeoclimatology Palaeoecology*, 163, 163–196.

Scheck-Wenderoth, M. & Lamarche, J. (2005) Crustal memory and basin evolution in the Central European Basin System—new insights from a 3D structural model. *Tectonophysics*, 397, 143–165.

Schwark, L. & Frimmel, A. (2004) Chemostratigraphy of the Posidonia Black Shale, SW-Germany: II. Assessment of extent and persistence of photic-zone anoxia using aryl isoprenoid distributions. *Chemical Geology*, 206, 231–248.

Schwark, L. & Ruebsam, W. (2024) Climate cyclicity-controlled recurrent bottom-water ventilation events in the aftermath of the Toarcian Oceanic Anoxic Event: the Jenkyns Event. *International Journal of Earth Sciences*, 113, 1–16.

Silva, R.L., Duarte, L.V., Wach, G., Ruhl, M., Sadki, D., Gómez, J., Hesselbo, S., Xu, W., O'connor, D. & Rodrigues, B. (2021) An Early Jurassic (Sinemurian–Toarcian) stratigraphic framework for the occurrence of organic matter preservation intervals (OMPIs). *Earth-Science Reviews*, 221, 103780.

Song, J.L., Littke, R. & Weniger, P. (2017) Organic geochemistry of the Lower Toarcian Posidonia Shale in NW Europe. *Organic Geochemistry*, 106, 76–92.

Song, J.L., Littke, R., Weniger, P., Ostertag-Henning, C. & Nelskamp, S. (2015) Shale oil potential and thermal maturity of the Lower

Toarcian Posidonia Shale in NW Europe. *International Journal of Coal Geology*, 150, 127–153.

Stein, R. (1986) Surface-water paleoproductivity as inferred from sediments deposited in oxic and anoxic deep-water environments of the Mesozoic Atlantic Ocean. *Mitteilungen Geologisch-Paläontologisches Institut, Universität Hamburg*, 60, 55–70.

Stock, A.T., Littke, R., Schwarzbauer, J., Horsfield, B. & Hartkopf-Fröder, C. (2017) Organic geochemistry and petrology of Posidonia Shale (Lower Toarcian, Western Europe)–The evolution from immature oil-prone to overmature dry gas-producing kerogen. *International Journal of Coal Geology*, 176, 36–48.

Stollhofen, H., Bachmann, G., Barnasch, J., Bayer, U., Beutler, G., Franz, M., Kästner, M., Legler, B., Mutterlose, J. & Radies, D. (2008) Upper Rotliegend to early cretaceous basin development. In: *Dynamics of complex intracontinental basins: the Central European Basin system*. Berlin: Springer, pp. 181–210.

Storm, M.S., Hesselbo, S.P., Jenkyns, H.C., Ruhl, M., Ullmann, C.V., Xu, W., Leng, M.J., Riding, J.B. & Gorbanenko, O. (2020) Orbital pacing and secular evolution of the Early Jurassic carbon cycle. *Proceedings of the National Academy of Sciences of the United States of America*, 117, 3974–3982.

Suan, G., Nikitenko, B.L., Rogov, M.A., Baudin, F., Spangenberg, J.E., Knyazev, V.G., Glinskikh, L.A., Goryacheva, A.A., Adatte, T. & Riding, J.B. (2011) Polar record of Early Jurassic massive carbon injection. *Earth and Planetary Science Letters*, 312, 102–113.

Suan, G., van de Schootbrugge, B., Adatte, T., Fiebig, J. & Oschmann, W. (2015) Calibrating the magnitude of the Toarcian carbon cycle perturbation. *Paleoceanography*, 30, 495–509.

Sundararaman, P., Schoell, M., Littke, R., Baker, D.R., Leythaeuser, D. & Rullkötter, J. (1993) Depositional environment of Toarcian Shales from Northern Germany as monitored with porphyrins. *Geochimica et Cosmochimica Acta*, 57, 4213–4218.

Svensen, H., Planke, S., Chevallier, L., Malthe-Sorenssen, A., Corfu, F. & Jamtveit, B. (2007) Hydrothermal venting of greenhouse gases triggering Early Jurassic global warming. *Earth and Planetary Science Letters*, 256, 554–566.

Sweere, T., van den Boorn, S., Dickson, A.J. & Reichart, G.-J. (2016) Definition of new trace-metal proxies for the controls on organic matter enrichment in marine sediments based on Mn, Co, Mo and Cd concentrations. *Chemical Geology*, 441, 235–245.

Taylor, G.H., Teichmüller, M., Davis, A., Diessel, C., Littke, R. & Robert, P. (1998) Organic petrology.

Them, T.R., Gill, B.C., Caruthers, A.H., Gröcke, D.R., Tulsky, E.T., Martindale, R.C., Poulton, T.P. & Smith, P.L. (2017) High-resolution carbon isotope records of the Toarcian Oceanic Anoxic Event (Early Jurassic) from North America and implications for the global drivers of the Toarcian carbon cycle. *Earth and Planetary Science Letters*, 459, 118–126.

Them, T.R., Gill, B.C., Selby, D., Gröcke, D.R., Friedman, R.M. & Owens, J.D. (2017) Evidence for rapid weathering response to climatic warming during the Toarcian Oceanic Anoxic Event. *Scientific Reports*, 7, 5003.

Thibault, N., Ruhl, M., Ullmann, C.V., Korte, C., Kemp, D.B., Gröcke, D.R. & Hesselbo, S.P. (2018) The wider context of the Lower Jurassic Toarcian oceanic anoxic event in Yorkshire coastal outcrops, UK. *Proceedings of the Geologists' Association*, 129, 372–391.

Togunwa, O.S. & Abdullah, W.H. (2017) Geochemical characterization of Neogene sediments from onshore West Baram Delta Province, Sarawak: paleoenvironment, source input and thermal maturity. *Open Geosciences*, 9, 302–313.

Tribovillard, N., Algeo, T.J., Lyons, T. & Riboulleau, A. (2006) Trace metals as paleoredox and paleoproductivity proxies: an update. *Chemical Geology*, 232, 12–32.

Turekian, K.K. & Wedepohl, K.H. (1961) Distribution of the elements in some major units of the earths crust. *Geological Society of America Bulletin*, 72, 175–191.

van de Schootbrugge, B., Bachan, A., Suan, G., Richoz, S. & Payne, J.L. (2013) Microbes, Mud and Methane: cause and consequence of recurrent Early Jurassic Anoxia following the End-Triassic mass extinction. *Palaeontology*, 56, 685–709.

van de Schootbrugge, B., Bailey, T.R., Rosenthal, Y., Katz, M.E., Wright, J.D., Miller, K.G., Feist-Burkhardt, S. & Falkowski, P.G. (2005) Early Jurassic climate change and the radiation of organic-walled phytoplankton in the Tethys Ocean. *Paleobiology*, 31, 73–97.

van de Schootbrugge, B., Richoz, S., Pross, J., Luppold, F.W., Hunze, S., Wonik, T., Blau, J., Meister, C., van der Weijst, C.M.H., Suan, G., Fraguas, A., Fiebig, J., Herrle, J.O., Guex, J., Little, C.T.S., Wignall, P.B., Püttmann, W. & Oschmann, W. (2019) The Schandelah Scientific Drilling Project: a 25-million year record of Early Jurassic palaeo-environmental change from northern Germany. *Newsletters on Stratigraphy*, 52, 249–296.

van Wees, J.D., Stephenson, R.A., Ziegler, P.A., Bayer, U., Mccann, T., Dadlez, R., Gaupp, R., Narkiewicz, M., Bitzer, F. & Scheck, M. (2000) On the origin of the Southern Permian Basin, Central Europe. *Marine and Petroleum Geology*, 17, 43–59.

Wang, Y., Ossa, F.O., Spangenberg, J.E., Wille, M. & Schoenberg, R. (2021) Restricted oxygen-deficient basins on the Northern European epicontinental shelf across the Toarcian carbon isotope excursion interval. *Paleoceanography and Paleoclimatology*, 36, e2020PA004207.

Wedepohl, K. (1971) Environmental influences on the chemical composition of shales and clays. *Physics and Chemistry of the Earth*, 8, 307–333.

Wedepohl, K. (1991) The composition of the upper earth's crust and the natural cycles of selected metals. Metal in natural raw materials, natural resources. In: *Metals and their compounds in the environment. Occurrence, analysis and biological relevance*. Hoboken: Wiley, pp. 3–17.

Wignall, P.B. (1991) Model for transgressive black shales. *Geology*, 19, 167–170.

Wignall, P.B. (2001) Large igneous provinces and mass extinctions. *Earth-Science Reviews*, 53, 1–33.

Wignall, P.B., Newton, R.J. & Little, C.T.S. (2005) The timing of paleoenvironmental change and cause-and-effect relationships during the early Jurassic mass extinction in Europe. *American Journal of Science*, 305, 1014–1032.

Wilkin, R., Barnes, H. & Brantley, S. (1996) The size distribution of framboidal pyrite in modern sediments: an indicator of redox conditions. *Geochimica et Cosmochimica Acta*, 60, 3897–3912.

Wu, Z., Littke, R., Guo, T., HE, S. & Grohmann, S. (2025) Organic matter accumulation, paleoenvironment and kerogen structure of the Middle Jurassic Dameigou Formation, Qaidam Basin: evidence from organic petrography and geochemistry. *International Journal of Coal Geology*, 300, 104707.

Wu, Z.R., Grohmann, S. & Littke, R. (2024) Geochemistry and petrology of Early Permian lacustrine shales in the Lod'eve Basin,

Southern France: depositional history, organic matter accumulation and thermal maturity. *International Journal of Coal Geology*, 284, 104469.

Xu, W.M., Ruhl, M., Jenkyns, H.C., Leng, M.J., Huggett, J.M., Minisini, D., Ullmann, C.V., Riding, J.B., Weijers, J.W.H., Storm, M.S., Percival, L.M.E., Tosca, N.J., Idiz, E.F., Tegelaar, E.W. & Hesselbo, S.P. (2018) Evolution of the Toarcian (Early Jurassic) carbon-cycle and global climatic controls on local sedimentary processes (Cardigan Bay Basin, UK). *Earth and Planetary Science Letters*, 484, 396–411.

Ziegler, P.A. (1990) *Geological atlas of western and central Europe*. The Hague: Shell Internationale Petroleum Maatschappij BV.

Zimmermann, J., Franz, M., Heunisch, C., Luppold, F.W., Monnig, E. & Wolfgramm, M. (2015) Sequence stratigraphic framework of the Lower and Middle Jurassic in the North German Basin: epicontinental sequences controlled by Boreal cycles. *Palaeogeography Palaeoclimatology Palaeoecology*, 440, 395–416.

SUPPORTING INFORMATION

Additional supporting information can be found online in the Supporting Information section at the end of this article.

How to cite this article: Wijesinghe, P., Littke, R., Burnaz, L., Blumenberg, M., Erbacher, J., Mann, T. et al. (2025) Black shale deposition during the Early Jurassic: Geochemistry of Pliensbachian and Toarcian sedimentary rocks of the Hunzen Well, Hils Syncline, Northwest German Basin. *The Depositional Record*, 00, 1–28. Available from: https://doi.org/10.1002/dep2.70037